Relativistic Jets at the Braking Point

Physical Properties of FR1 Jets from the VLA and Chandra

Alan Bridle (NRAO)

Colleagues

Robert Laing (ESO/ALMA)
James Canvin (U.Sydney)
Bill Cotton (NRAO)

X-ray imaging:
Judith Croston (U.Herts)
Martin Hardcastle (U.Herts)
Mark Birkinshaw (Bristol)
Diana Worrall (Bristol)

Outline

- FR1 and FR2 jets – the questions
- Why decelerating-jet models for FR1 jets?
- FR1 jet kinematics
- FR1 jet field configurations
- FR1 jet mass fluxes and entrainment
- Adiabats and particle acceleration
- Implications for FR2 jets

- What next?

AGN Jet Engine: B++

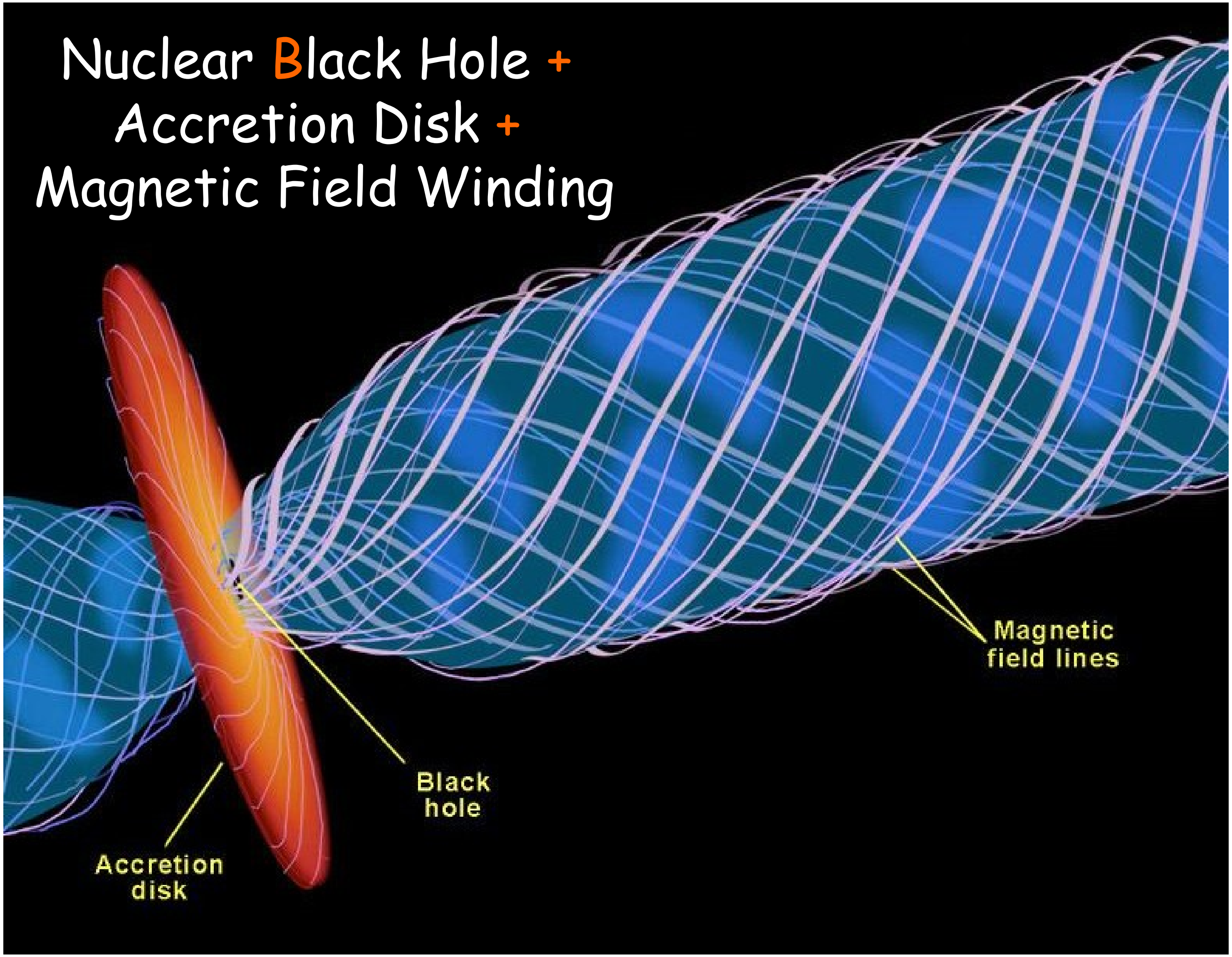

Fanaroff/Riley Types

- Original distinction: radio morphology

  source edge-darkened (Type 1)
vs
source edge-brightened (Type 2)

  Fanaroff and Riley, MNRAS 167, 31P (1974)

- Correlation with radio power

- Later: types correlate with two radio jet "flavors":

  collimation (1:wide, 2:narrow),
symmetry (1: more symmetric),
prominence (1: more prominent),
apparent B field (1: parallel → perp, 2: parallel to jet axis)

  Bridle, AJ 89, 979 (1984)

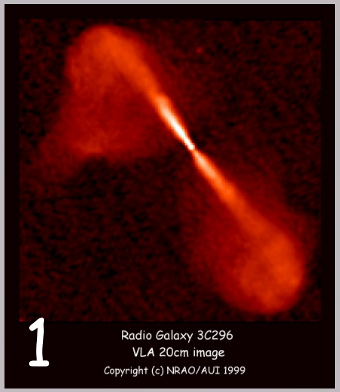

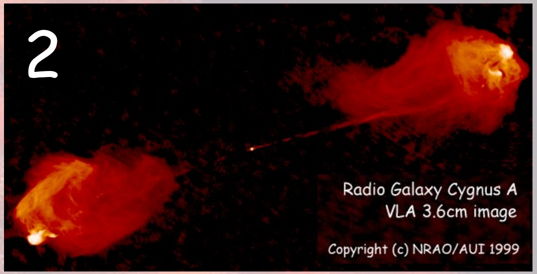

Strong Flavor Jets (FR2) → LOBES

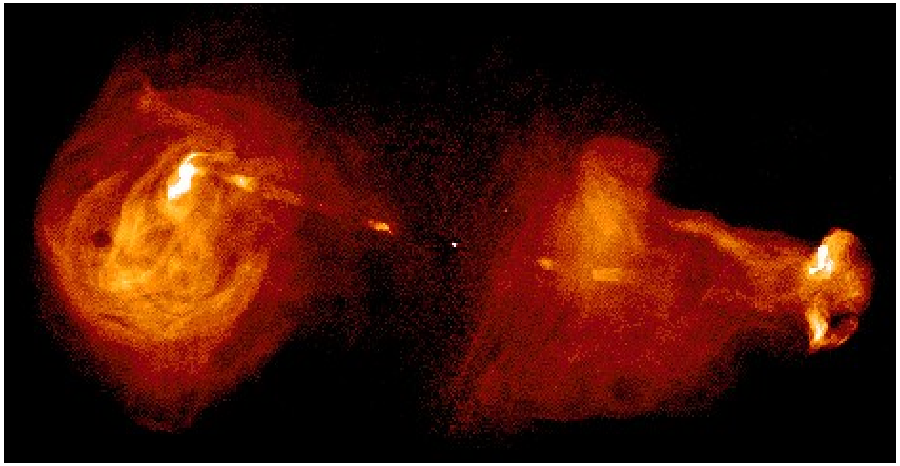

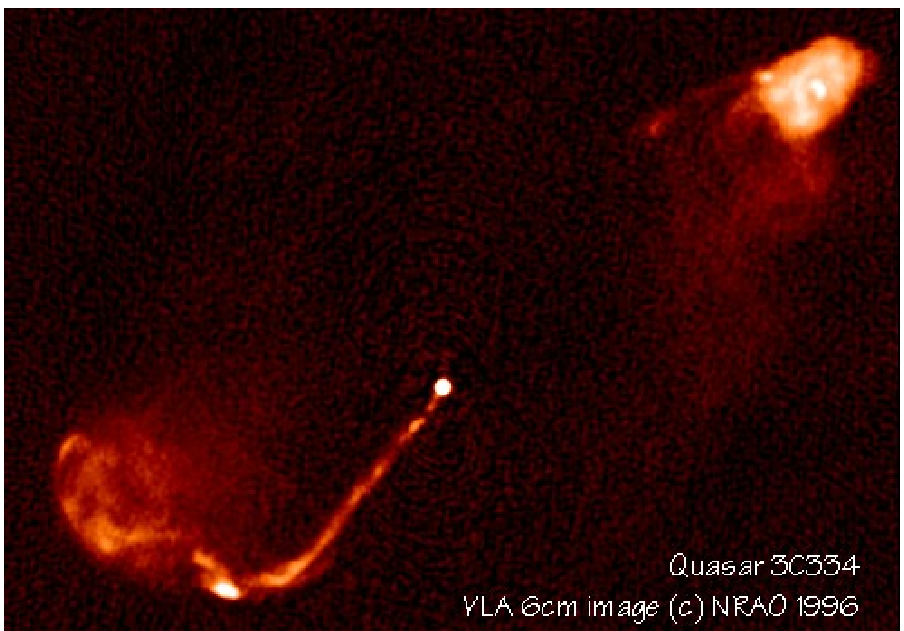

Narrow jets in powerful sources propagate supersonically to "hot spot" working surfaces where they decelerate and deflect, forming large "lobes" and "cocoons"

"One-sided" jets but two-sided lobes → FR2 jets stay at least mildly relativistic until final deceleration?

Weak Flavor Jets (FR1) → PLUMES

initially "one-sided" jets symmetrize

300 kpc field, 1.9 kpc FWHM 40 kpc field, 85 pc FWHM

3C31
1.4
GHz

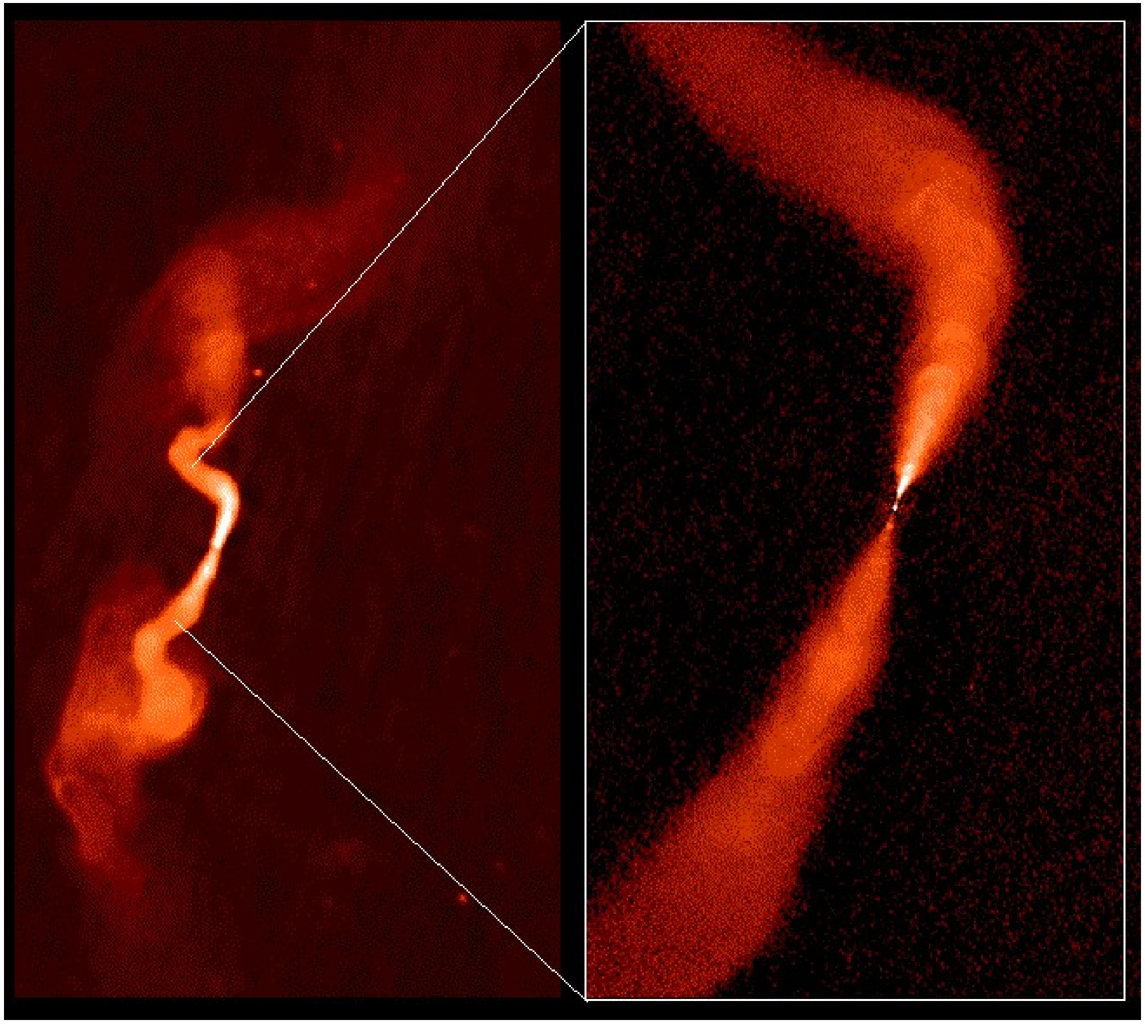

3C31
8.4
GHz

FR1/2 division: power+environment

1.4 GHz power

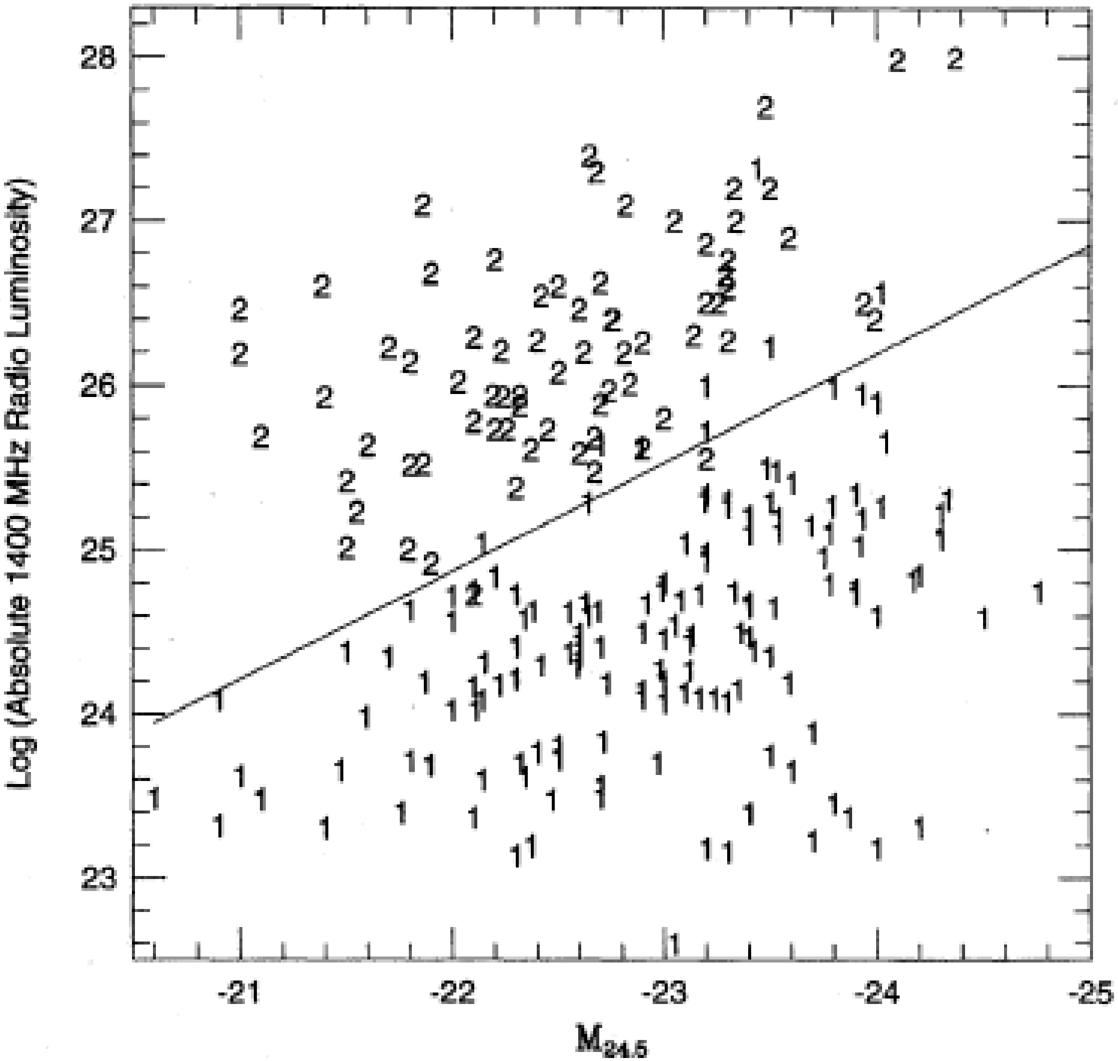

Ledlow & Owen (1996)

Optical luminosity (mass) of host galaxy

FR1 example: NGC315

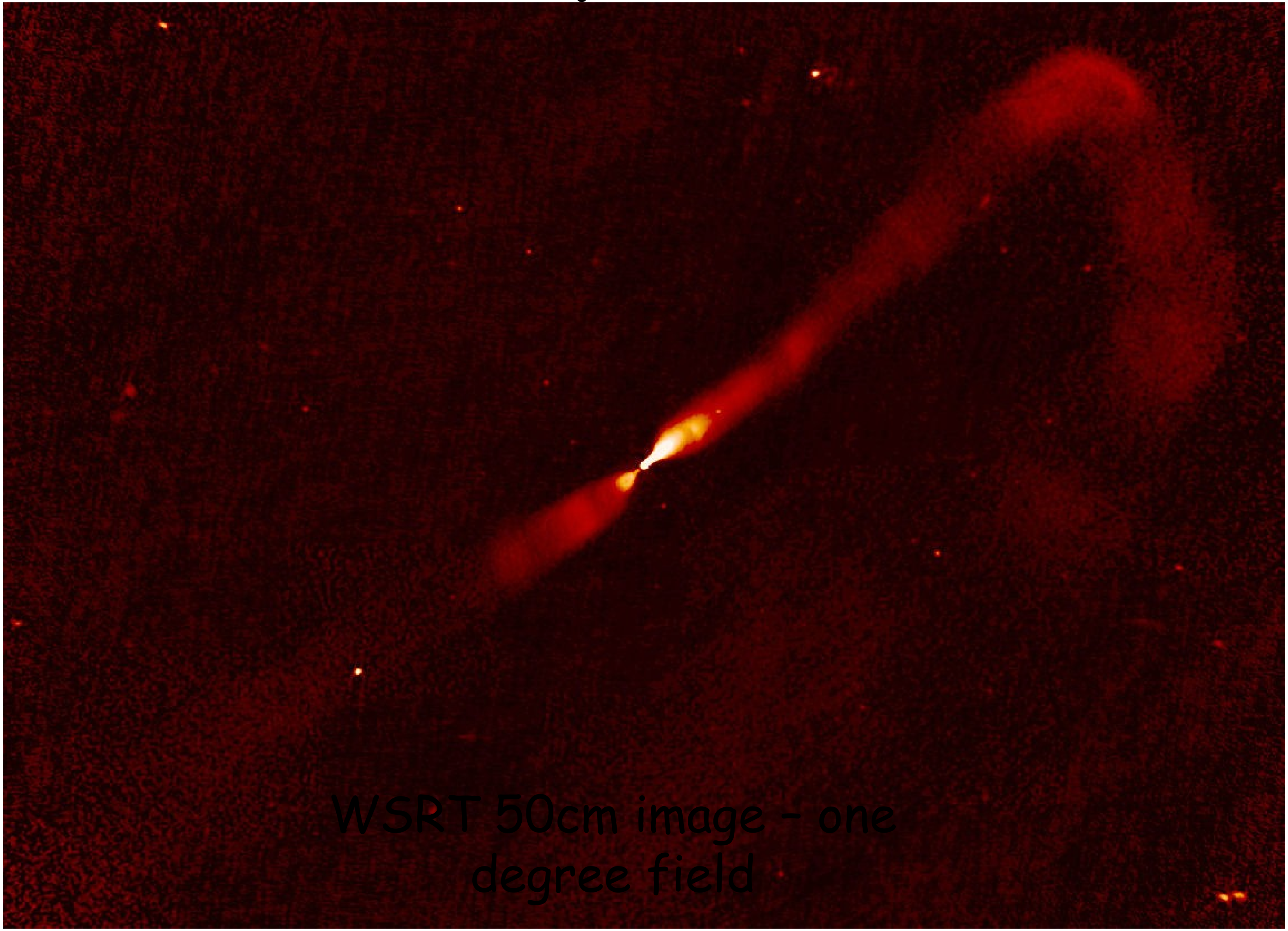

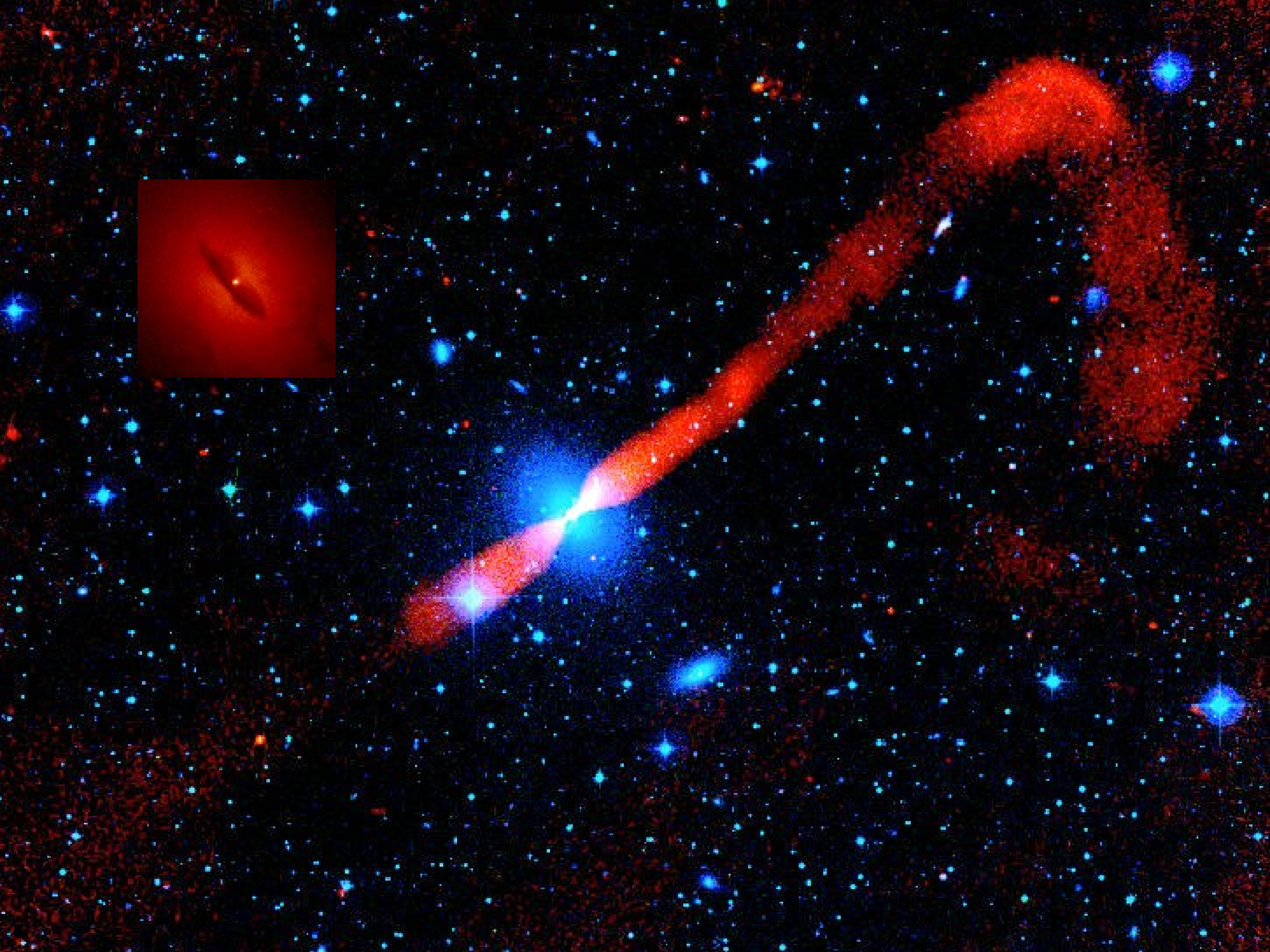

FR1 example 3C31=NGC383

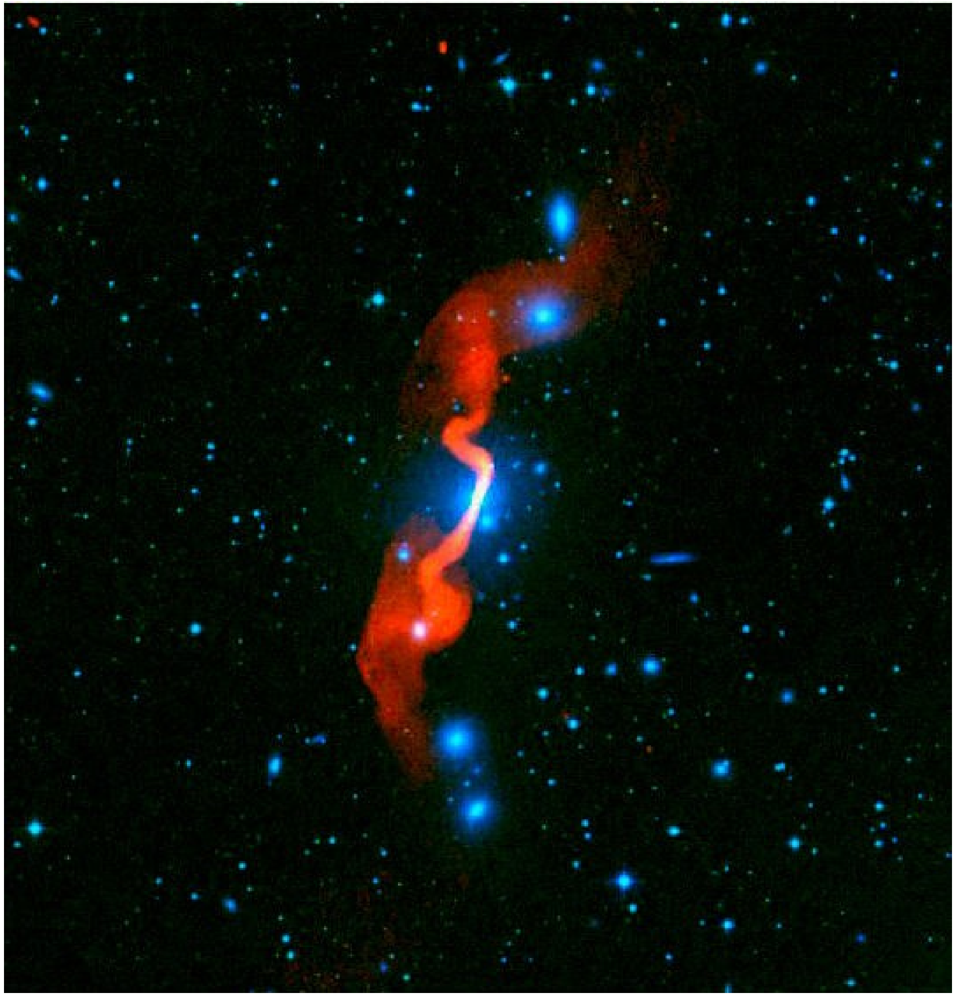

Red: VLA radio image
Blue: Optical image

Kpc-scale dust is common in nearby radio galaxies

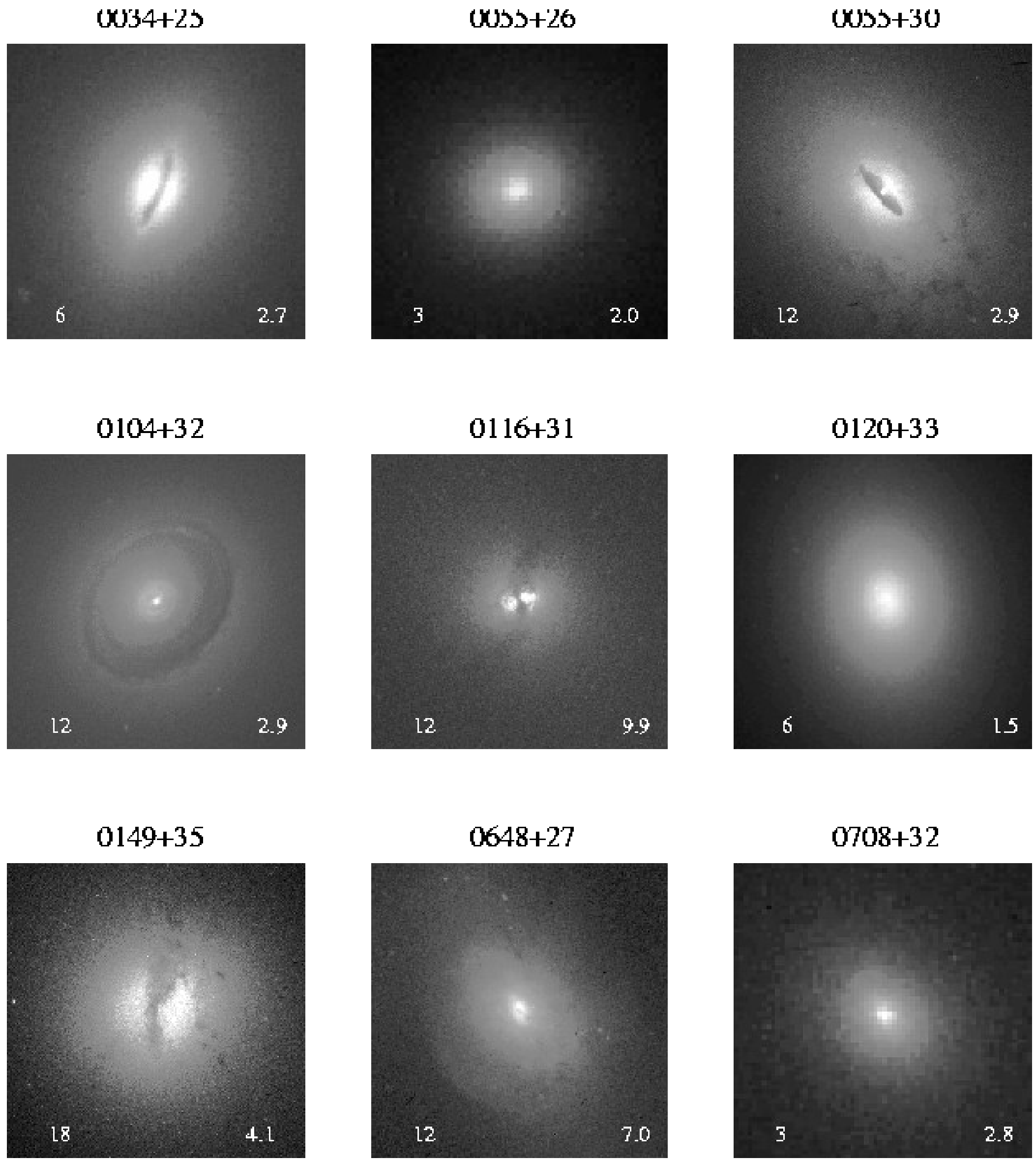

←NGC 315

3C 31 = NGC383 →

HST/WFPC2 imaging

Capetti et al., A&A 362, 871 (2000)

NGC383 Dust/CO

- major axis of dust "disk" about 2.5 kpc
- CO emission → ~10^9 solar masses of molecular gas within 1 kpc

[Okuda et al. ApJ 620, 673, 2005]

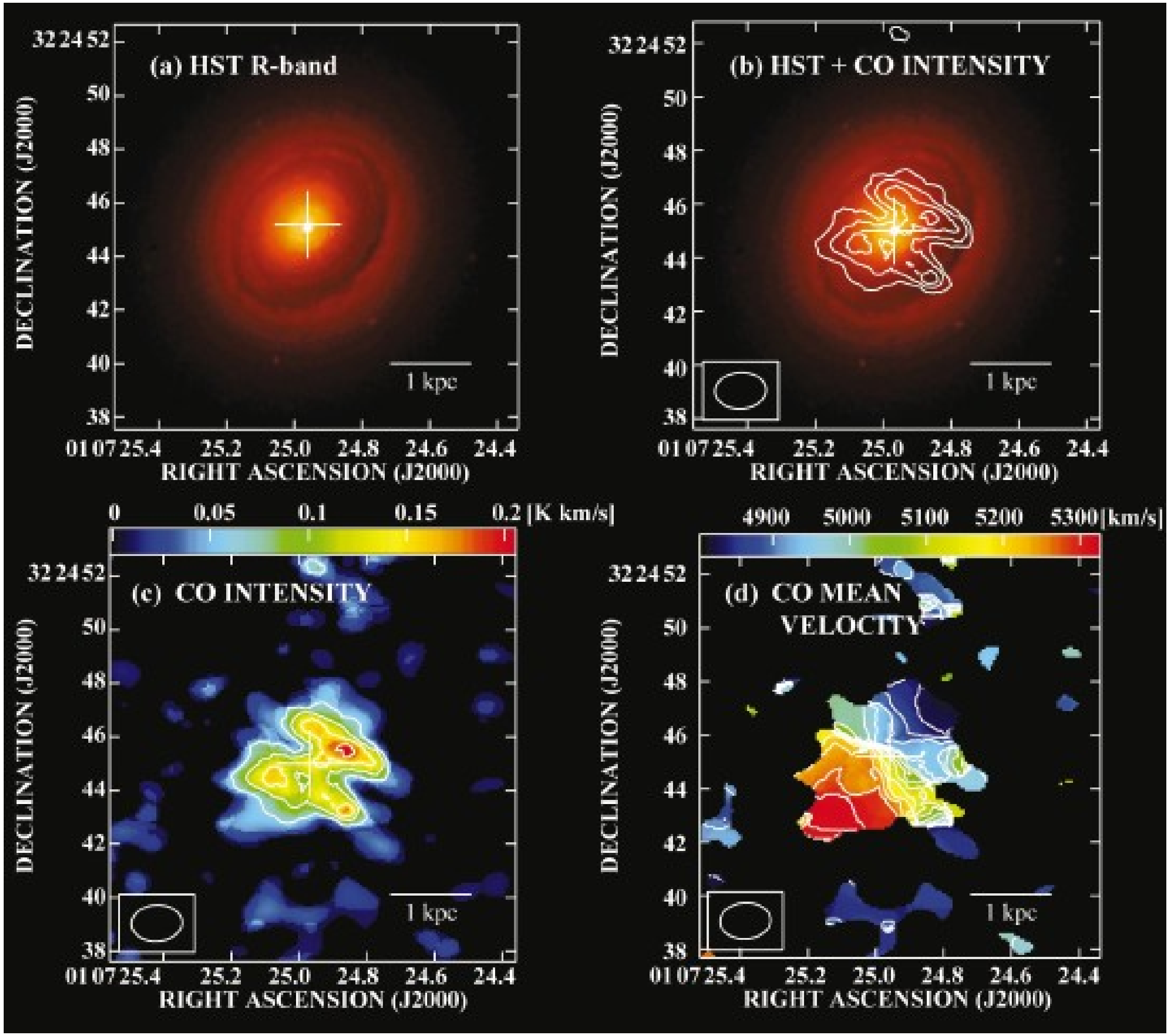

NGC383 Group-Scale Gas
1.7 x 10^7K atmosphere

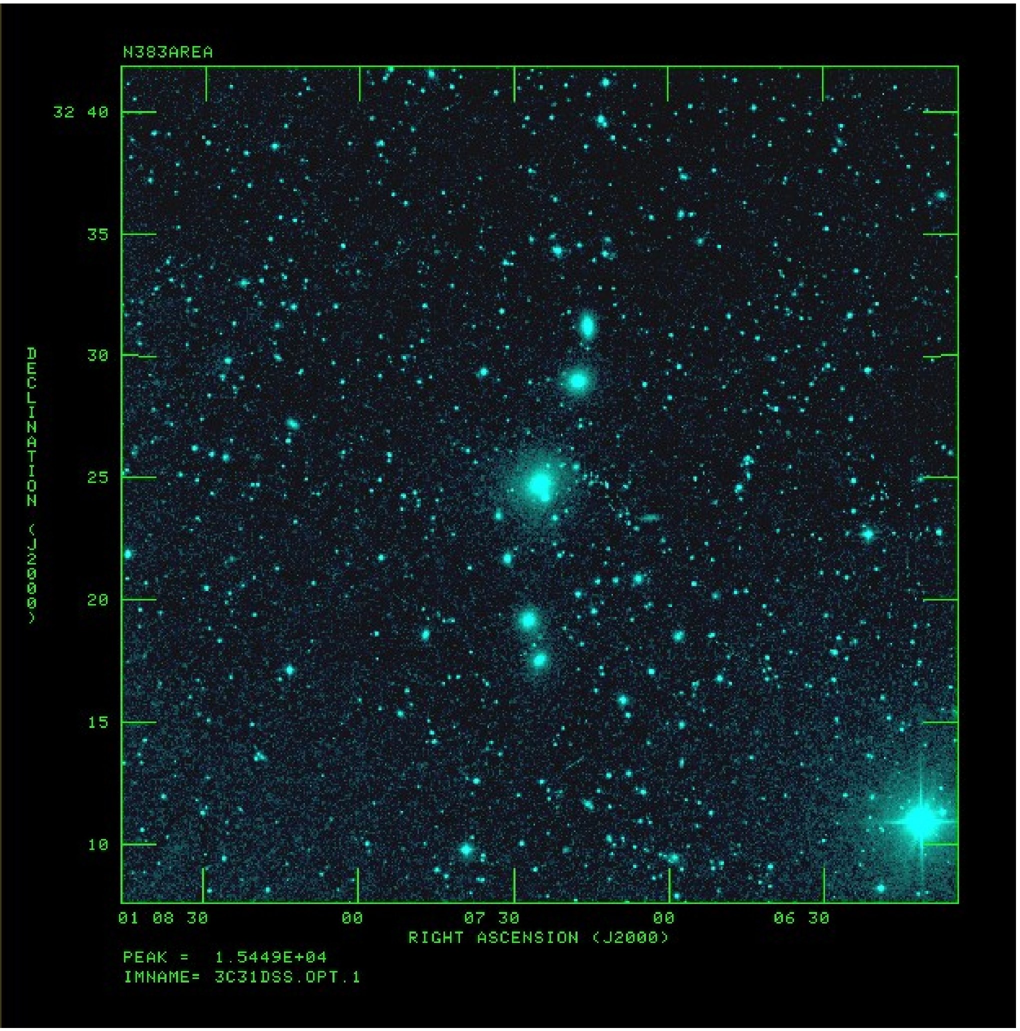

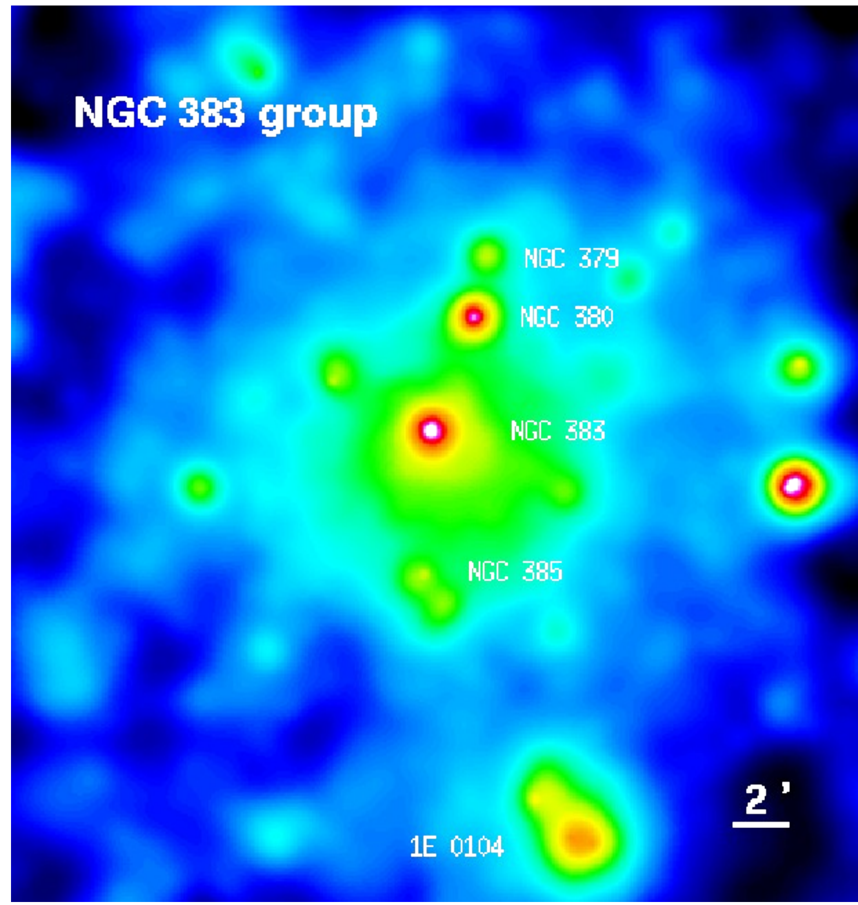

ROSAT PSPC image
Komossa and Bohringer A&A, 344, 755 (1999)

FR1 jets relativistic on pc scales …

- Direct detection of superluminal motion in some FR1 sources (VLBI)
- Relativistic potential well → expect bulk-relativistic outflow
- Unified models → parent population of BL Lac objects (intrinsically low-power blazars) with multiple bulk-relativistic jet signatures:
  - High brightness temperatures
  - Rapid variability
  - Variable γ-ray emission

… and remain fast on 1-kpc scales

- Proper motions in nearby galaxies: superluminal (M87); 0.5c (Cen A)
- Kpc-scale jet sidedness correlates with other indicators of bulk relativistic motion:
  - With fractional flux density in flat-spectrum radio "core"
  - With Faraday RM/depolarization asymmetry, apparently brighter jet base is on nearer (less rotated/depolarized) side of source if asymmetry large

Superluminal motion on kpc scale

M87 (Biretta, Zhou & Owen 1995)

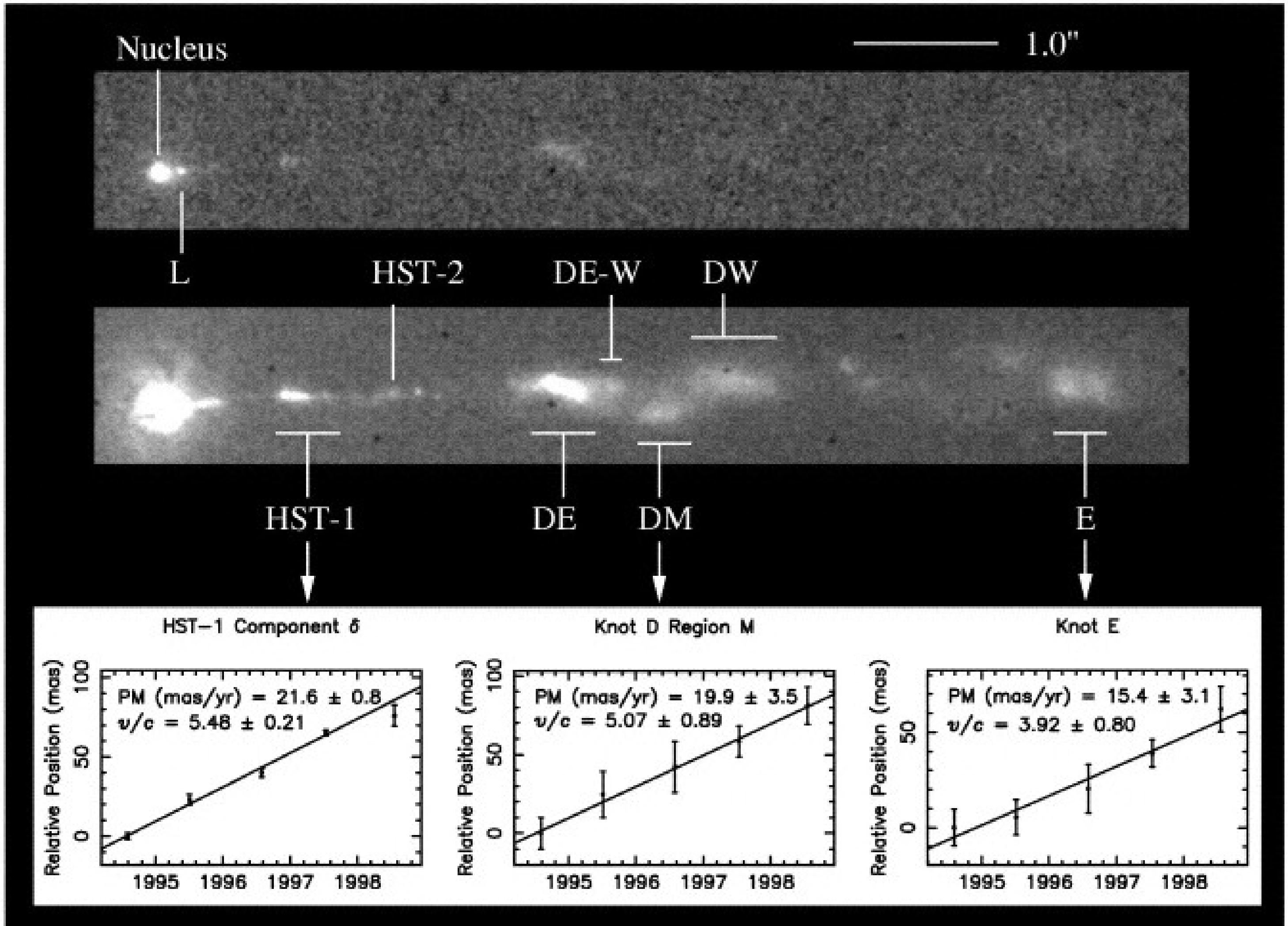

Cen A – nearest radio galaxy

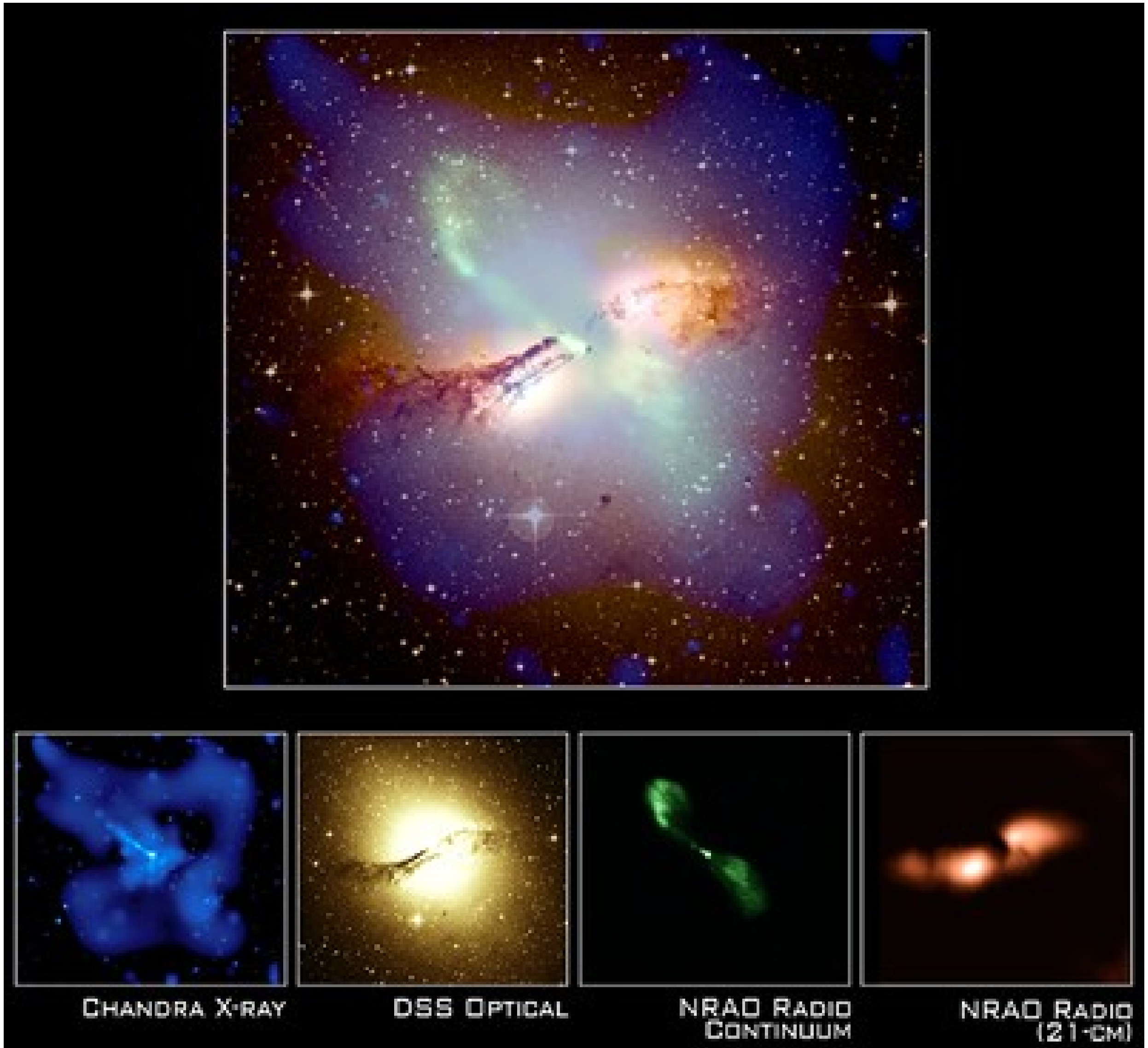

Cen A - proper motions on 100-pc scale

Knot motions at up to 0.5c between 1991 and 2002

VLA 8.4 GHz, Hardcastle et al. ApJ 593, 169 (2003)

Velocity evolution in FR1/2 jets?

- Both types start "fast" on sub-kpc scales …
- FR1 jets decelerate → slow, subsonic plumes FR2 jets stay fast, supersonic → hot spots
- Kinematics – where and how rapid is the deceleration?
- Dynamics - what and where are the interactions that decelerate FR1 jets?

- What can FR1 jet deceleration (braking) tell us about jet propagation within the host galaxy?

Modeling FR1 jet deceleration

- Assume intrinsically **symmetrical**, **axisymmetric**, **decelerating relativistic flows** with specified B-fields.
[How much of what we see in jet structures, symmetries, can be accounted for this way?]
- Derive best-fit functional forms for 3-D **velocity**, **emissivity and B-field geometry**.
[Fit “free models” to deep, high-resolution VLA images in total and linear polarized emission]
- Use **conservation of mass**, **momentum and energy** to infer variations of pressure, density, entrainment rate and Mach number in jets. [Get ambient gas density, pressure from X-ray data on galaxy, group atmospheres]
- Compare with **adiabatic models** to identify where jet emissivity variations require B-field amplification or relativistic particle injection/acceleration [compare with high-resolution images at short wavelengths.]

Relativistic jet modeling - Stokes I

Predicted radio intensity from slowing relativistic twin-jet

Observed VLA data for 3C31

NB "free-fit" model, no jet physics!

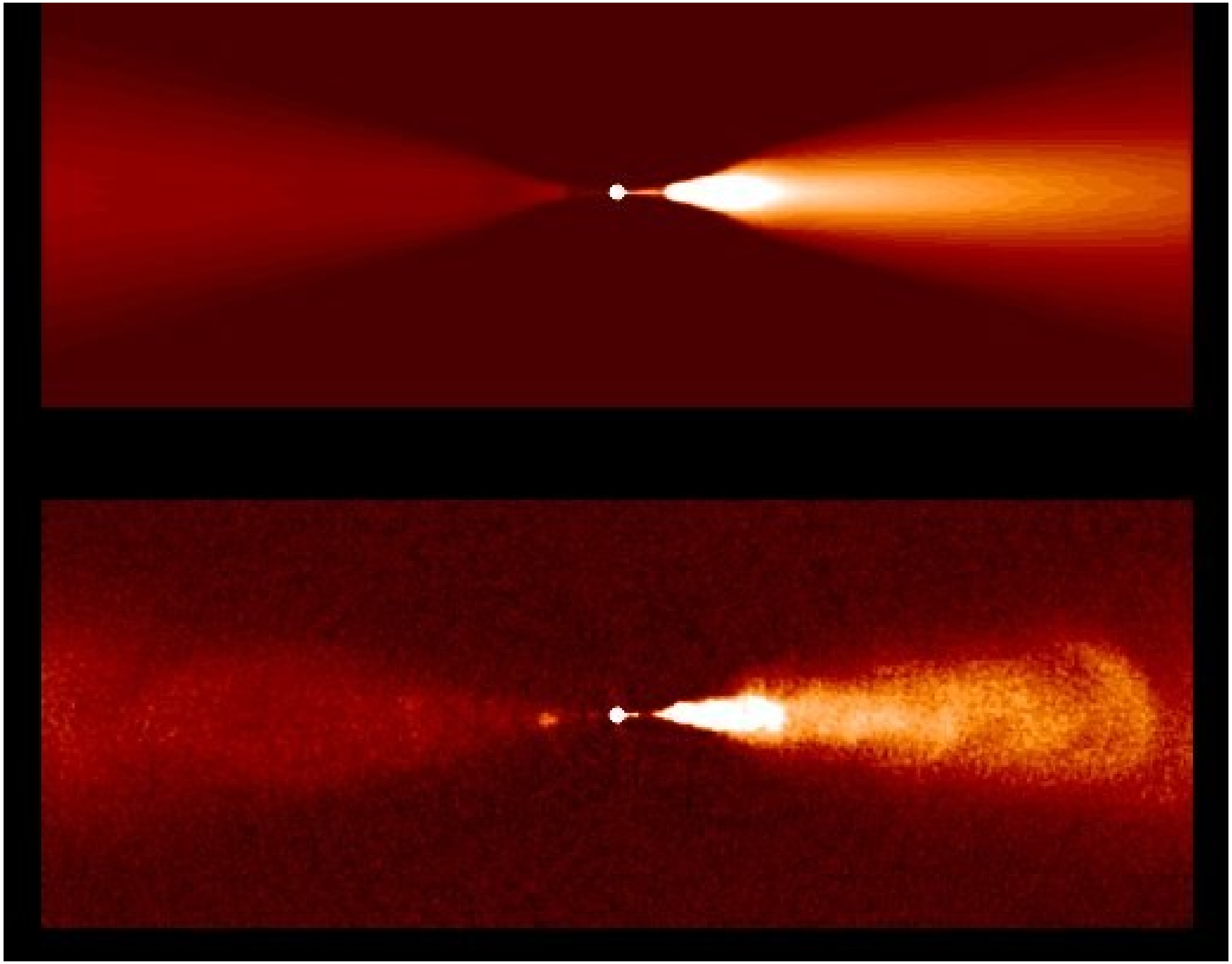

Angle/velocity degeneracy

Intensity Asymmetry:

$$\frac{I_j}{I_{cj}} = \left(\frac{1+\beta\cos\theta}{1-\beta\cos\theta}\right)^{2+\alpha}$$

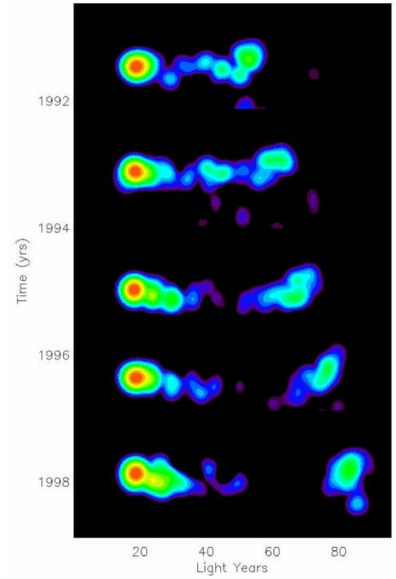

VLB jets – we can use superluminal motions to solve for velocity and angle for given I asymmetry, assuming relation between pattern and flow speed.

Cannot use on kpc scales, but there is another way!

Relativistic Aberration
between jet rest frame (′) and observed frame:

$$\sin\theta'_j = [\Gamma(1-\beta\cos\theta)]^{-1}\sin\theta \qquad \text{(main jet)},$$
$$\sin\theta'_{cj} = [\Gamma(1+\beta\cos\theta)]^{-1}\sin\theta \qquad \text{(counter-jet)}.$$

Aberration modifies polarization produced by given B-field in jets. Well-resolved polarimetry and B-field model can be used to **break degeneracy** by fitting jet/cjet asymmetries in Stokes Q and U.

Details of model fitting: Laing and Bridle, MNRAS 336, 328 (2002)

Moving objects appear rotated

Static tram

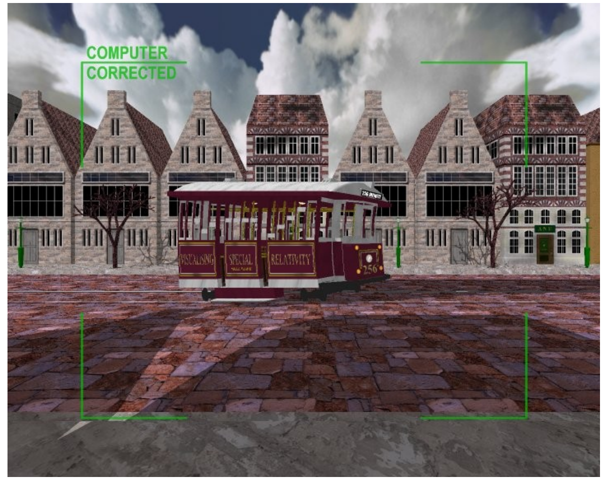

Effects of aberration

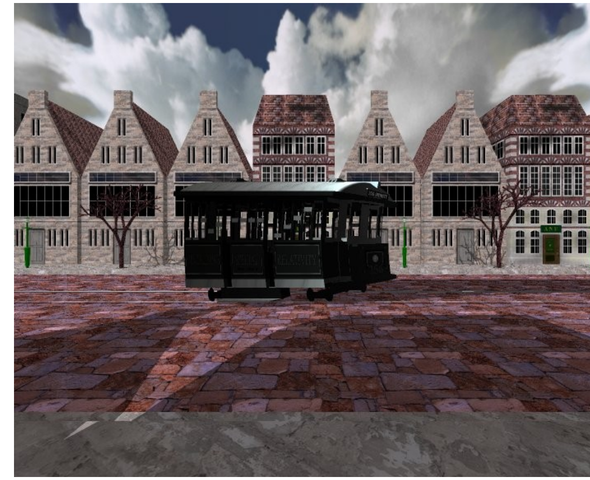

Aberration + Doppler

Rotation can be understood as an effect of relativistic aberration, or as a combination of Lorentz contraction and light-travel time (Terrell 1959; Penrose 1959)

“Visualising Special Relativity” (ANU Dept of Physics)
velocity 0.866c

Example – Synchrotron emission from a 2D random field sheet

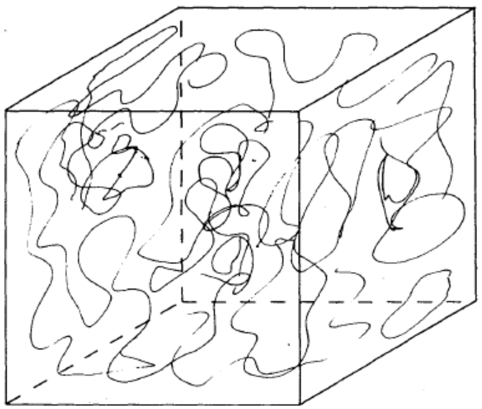

(a)

Before Compression

(b)

After Compression

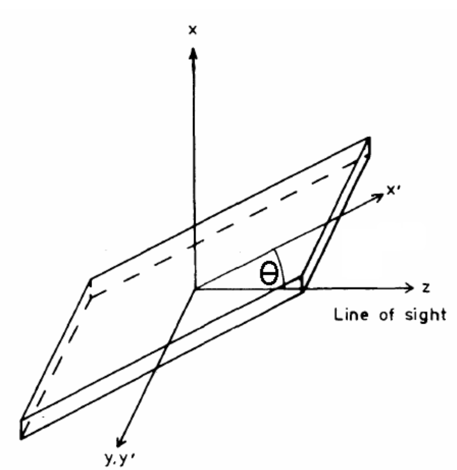

→

$$I = C(1 + \sin^2\theta)$$

$$Q = \tfrac{3}{4}C\cos^2\theta$$

for sp.index 1

Field Sheet Geometries and Jet Polarization Asymmetries

2D sheets perpendicular to jet axis
+ longitudinal-field shear layer

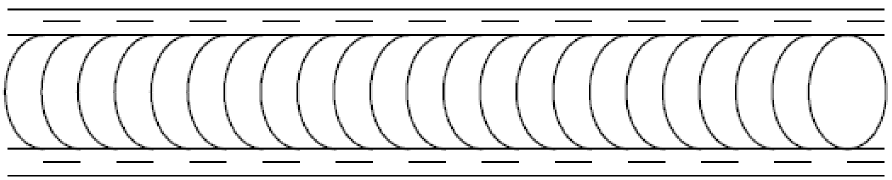

2D field sheets wrapped around jet axis
no radial, but toroidal + longitudinal cpts

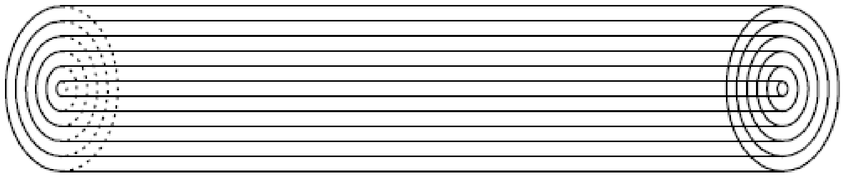

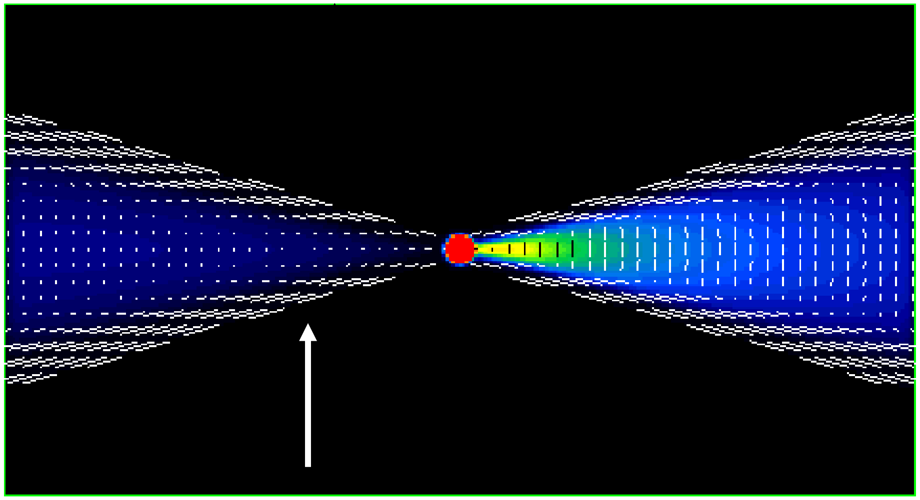

Apparent field transition in counter jet
NOT observed

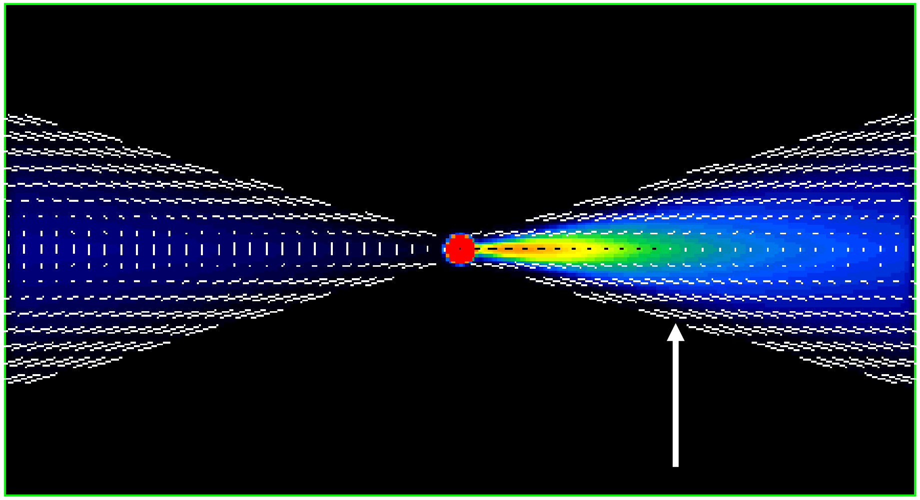

Field transition in main jet
IS observed

Model: decelerating relativistic jet with transverse velocity gradients

What goes INTO our models

- Observed jet geometry (given, not dynamical)
- VLA Stokes I,Q,U imaging at 1000's of pixels/jet
- Initial guesses for functional forms of:
  - Intrinsic emissivity (free power law or adiabats)
  - Velocity fields (longitudinal and transverse)
  - B-field component probability densities (free/adiabats) resembling wrapped-sheet configuration, varied to get fit
- Line of sight integrator for Stokes I,Q,U with relativistic beaming/aberration in actual field geometries
- I,Q,U chi-squared minimizer around initial guesses

What comes OUT of our models

- Best fits, error ranges for:
  1. Velocity field
  2. Inclination of jets to line of sight
  3. Magnetic field organization (orderliness)
  4. Emissivity variation along/across jets
- Goodness of fit measures
- Model images

Total intensity fitting

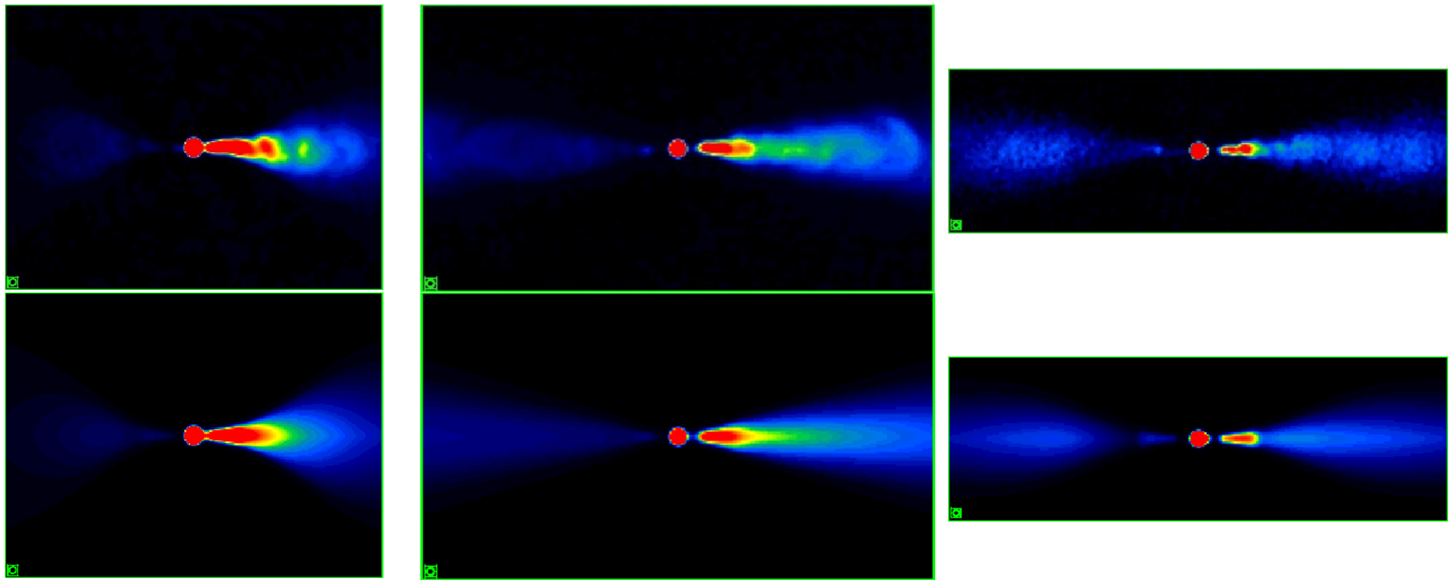

θ	38^o	52^o	64^o
	NGC 315	3C 31	B2 0326+39

% linear polarization

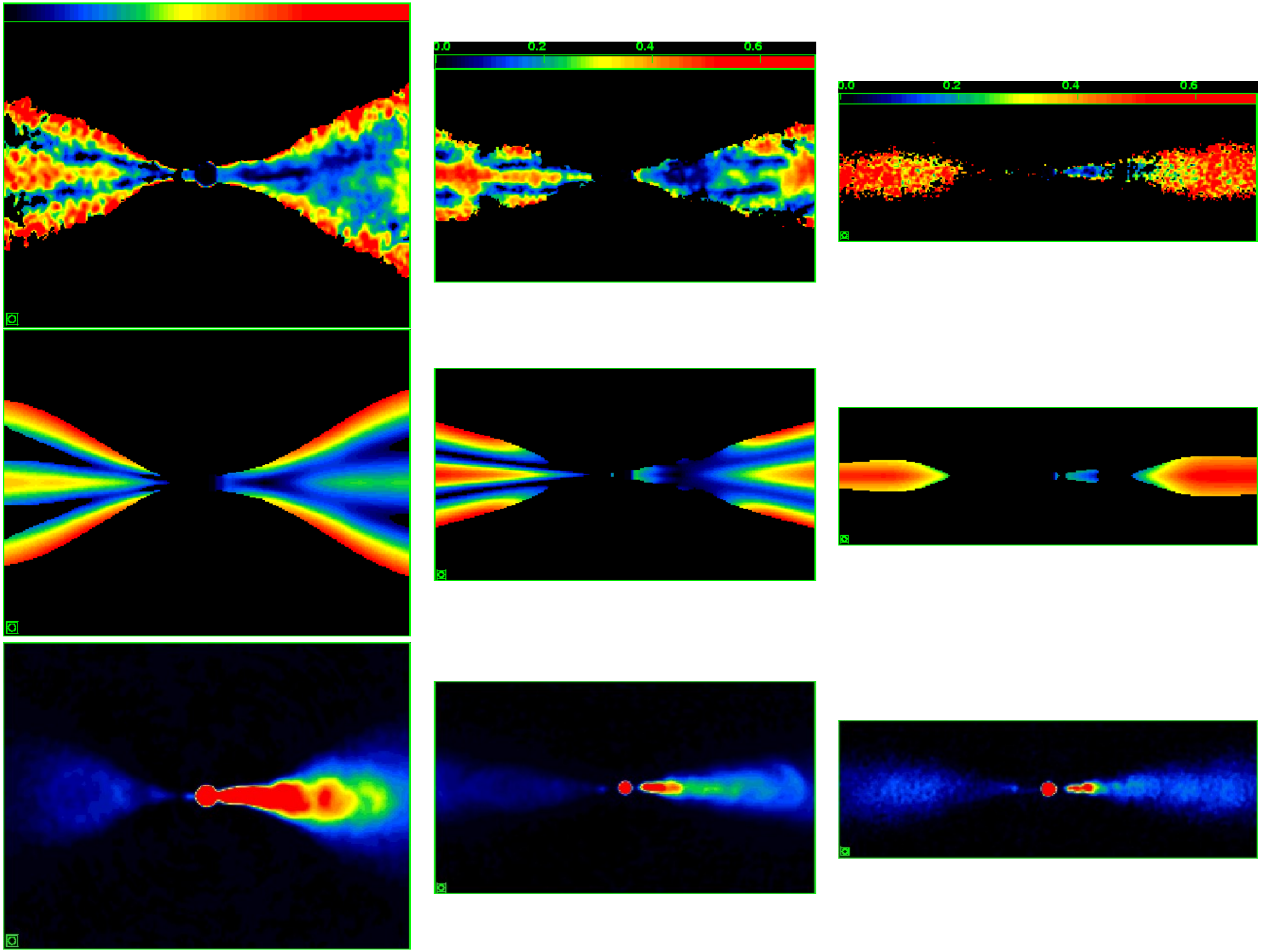

θ 38° (NGC315) 52° (3C31) 64° (B20326+39)

Modeled FR1 jet velocity fields

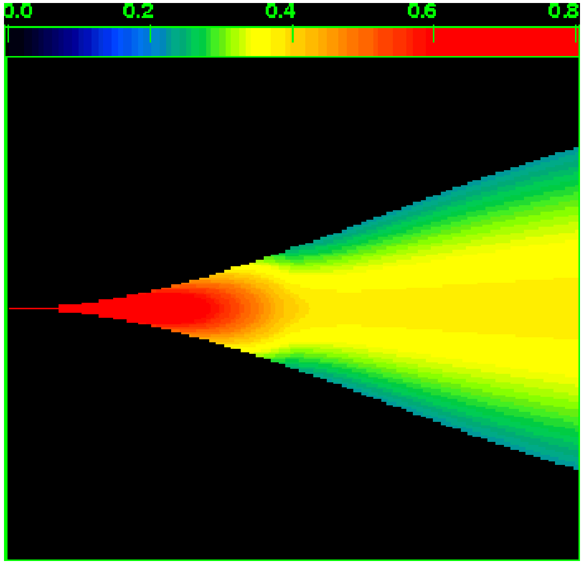

NGC 315

Canvin, Laing, Bridle & Cotton MNRAS **363**, 1223 (2005)

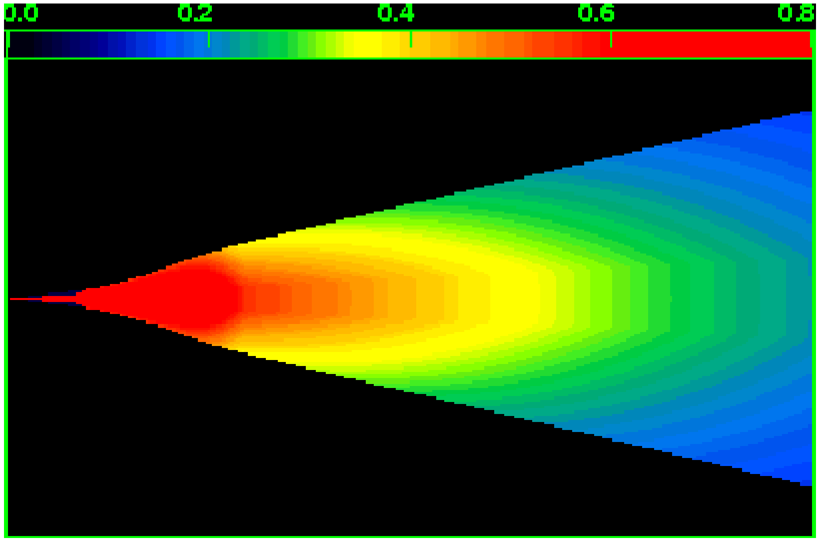

3C 31

Laing & Bridle, MNRAS **326**, 338 (2002)

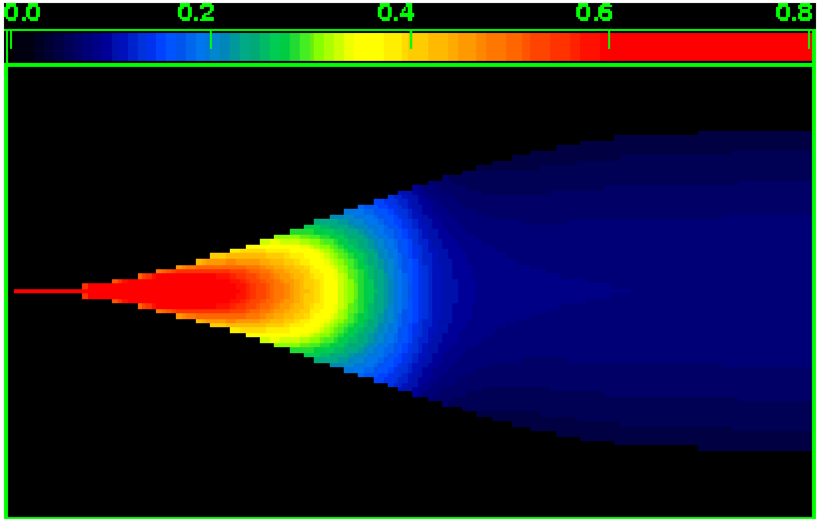

Typical ratio of edge to on-axis velocity ≈ 0.7

B2 0326+39

Canvin & Laing, MNRAS **350**, 1342 (2004)

Apparent B-field fitting: NGC315

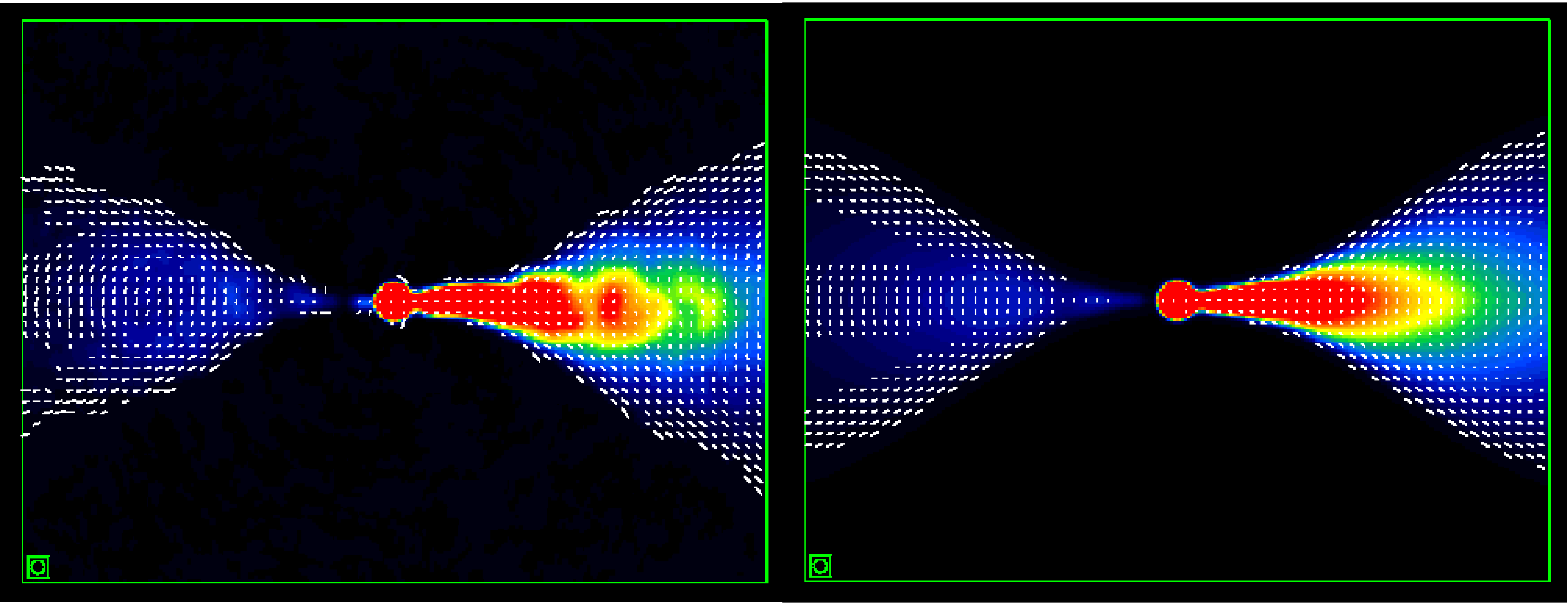

Data Model

vector length measures % poln

B-Field Component Evolution: NGC315

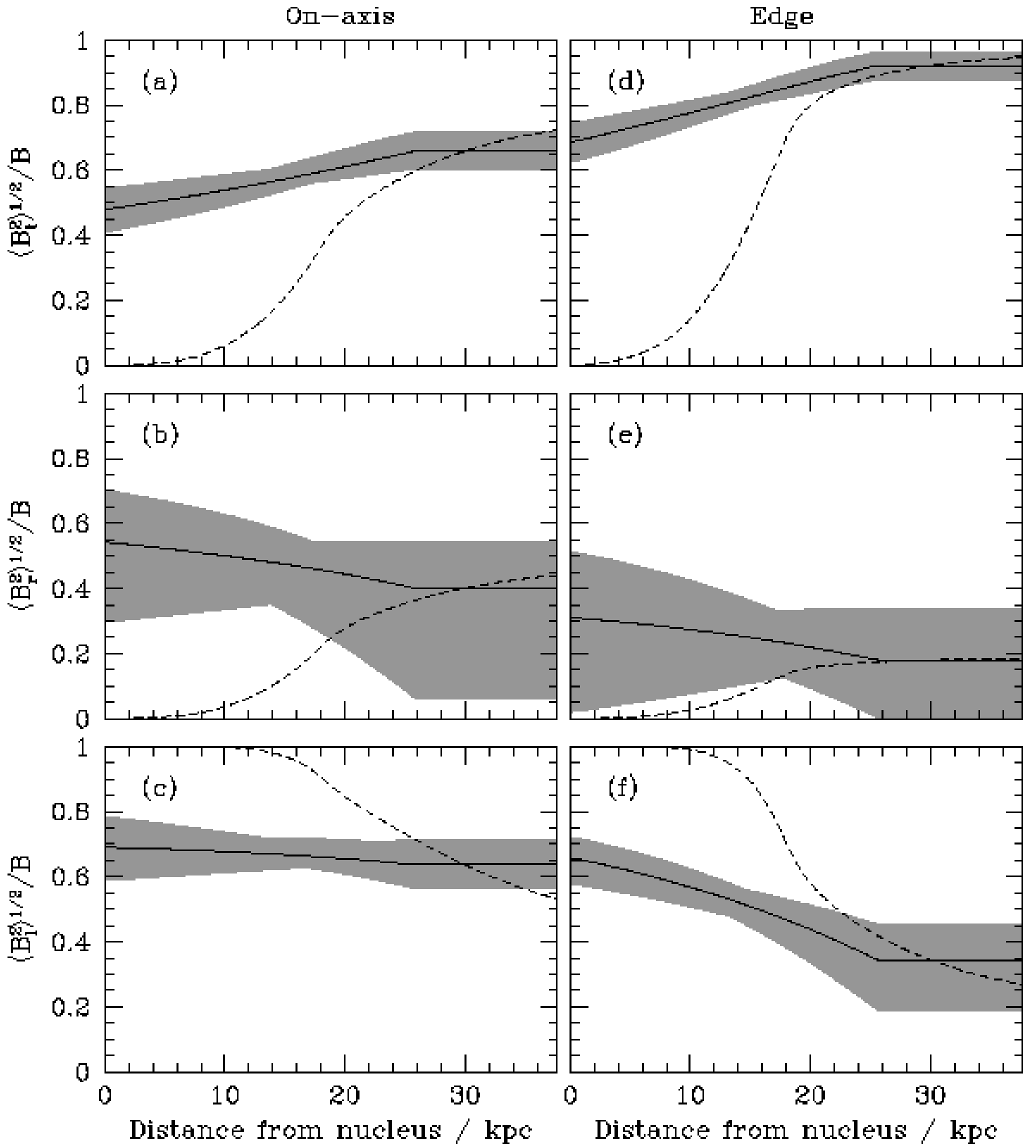

Toroidal

Radial

Longitudinal

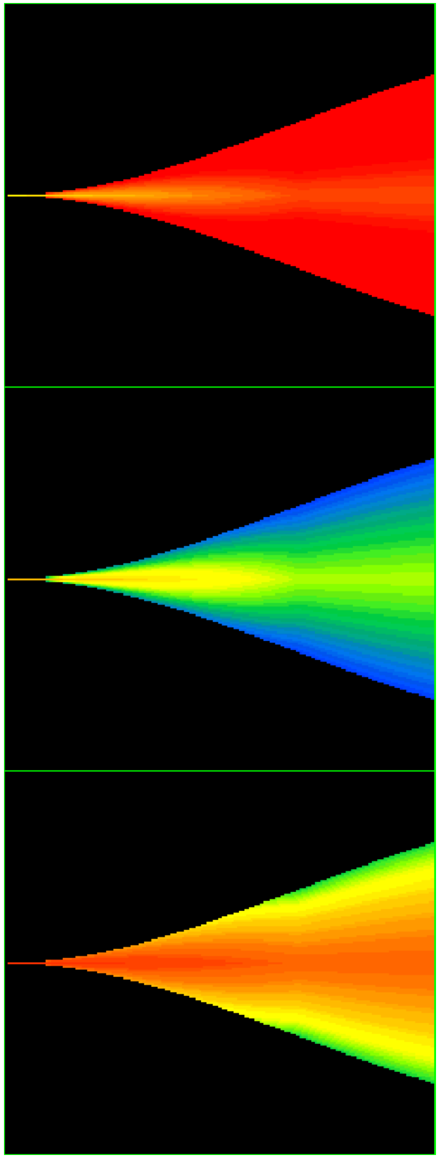

solid line – model fit, dashed line - frozen-in

Apparent B-field fitting: 3C31, B2 0326+39

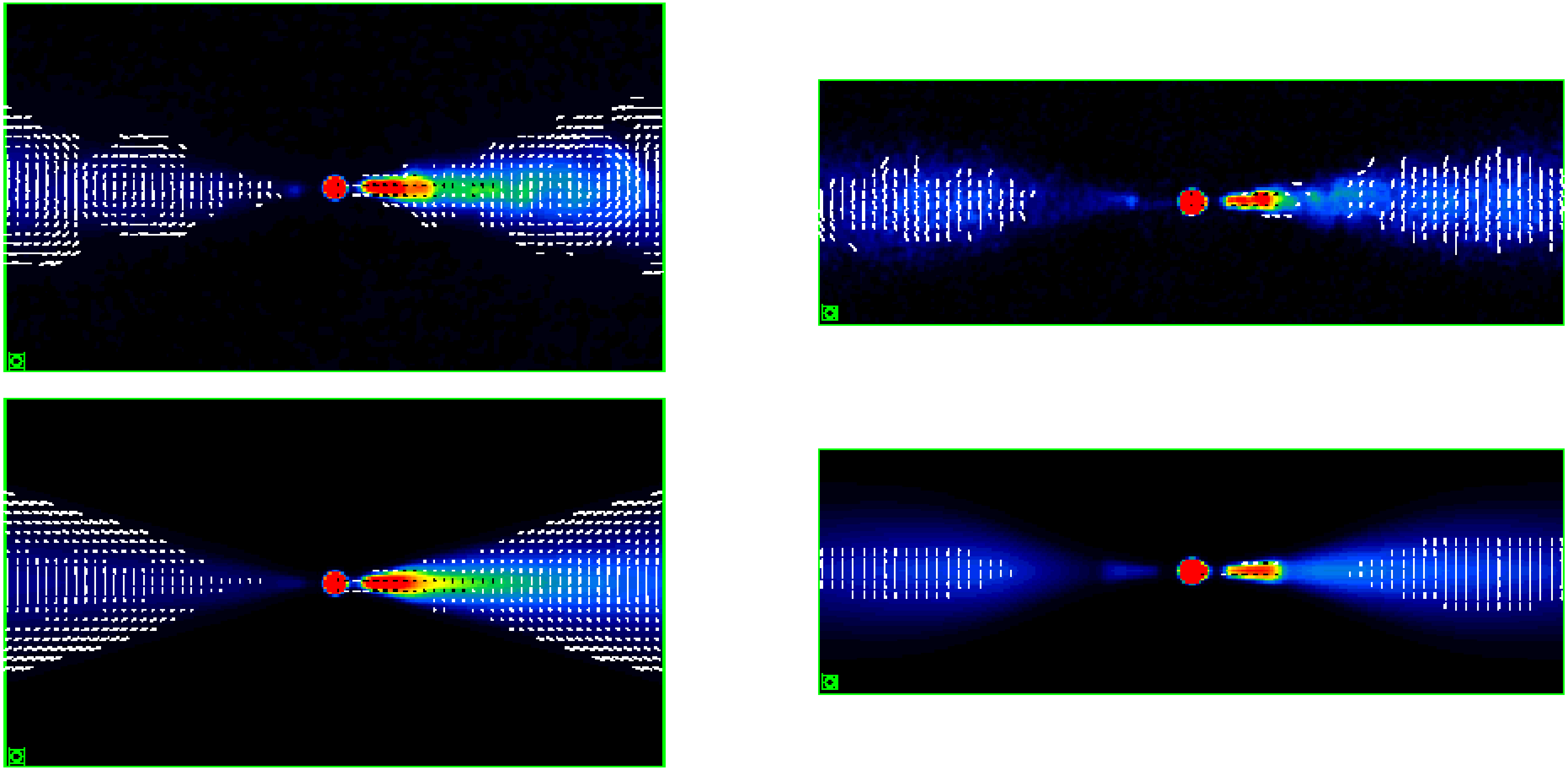

θ = 52° 64°

FR1 Jet B-field conclusions

- Models with pure transverse (i.e. radial+toroidal) field spine surrounded by pure longitudinal-field sheath predict B-field transition seen closer to nucleus in the approaching jet
  – not observed!
- Fitted field always primarily toroidal + longitudinal, with smaller radial components (as if velocity shear suppresses) evolving from mostly longitudinal close in towards mostly-toroidal further out, ~ equal at flare.
- Toroidal component *could* be ordered, provided the longitudinal field component has *many reversals* (unlike large-scale helical field)

N.B. Why not vector-ordered fields?

- Fields are not vector-ordered helices.
- Nor should we expect them to be:
  poloidal flux $\propto r^{-2}$;
  transverse flux $\propto (\Gamma\beta r)^{-1}$
- We do NOT see large-scale helical-field signatures - no transverse intensity asymmetries correlated with polarization structure asymmetries
- RM gradient "evidence" for helical fields specious? (but that's another story!)

Emission From Pure Helical Magnetic Fields

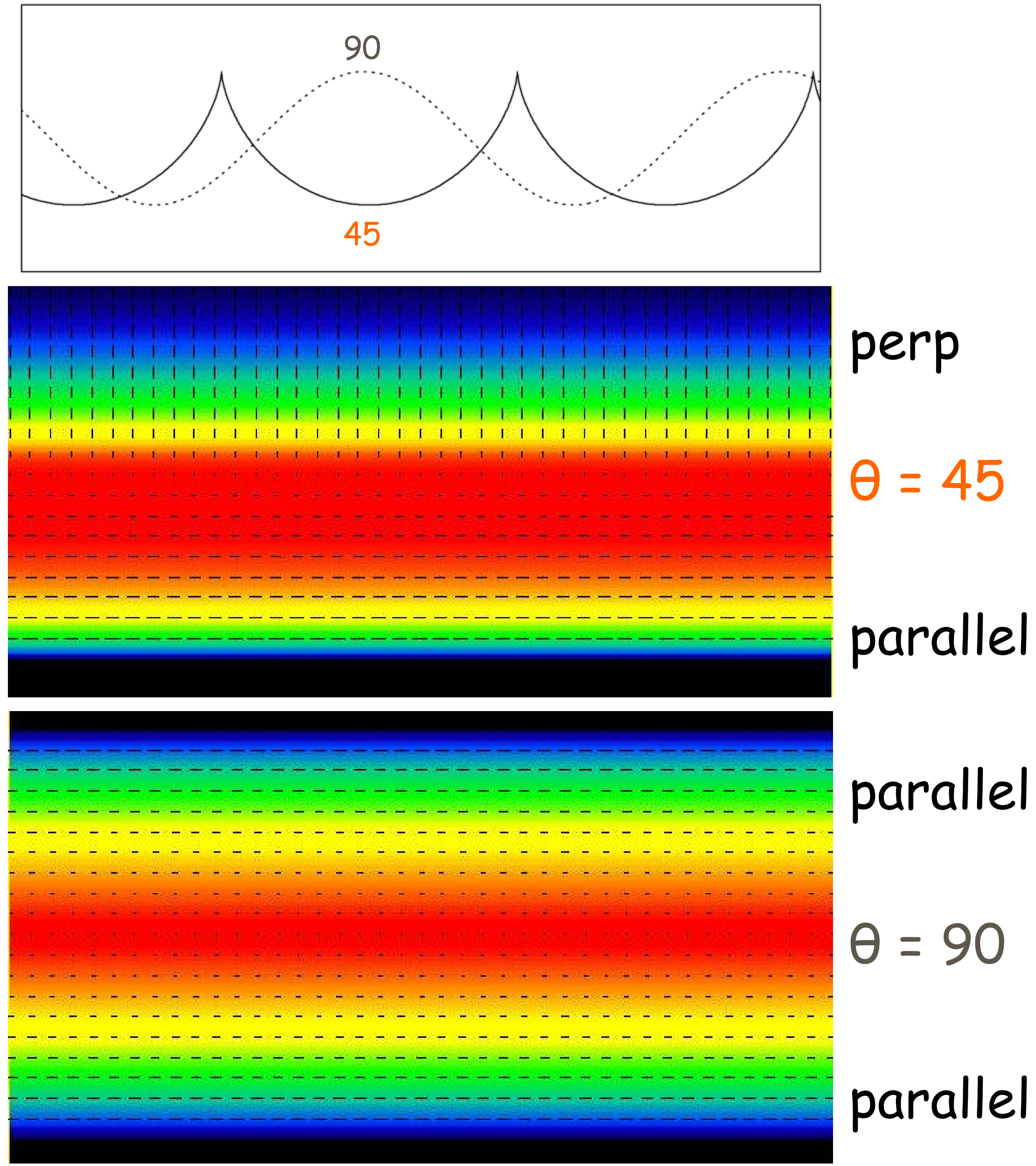

Jet Dynamics – Entrainment

CONCLUDE: Modeling well-resolved VLA intensity and polarization data can be used to show how FR1 jets decelerate on kpc scales

but it does not say why
… radio data alone give jet kinematics, not dynamics …

Extra step: X-ray data on gaseous environs of jets
Chandra/ROSAT/XMM

Chandra X-ray images of NGC383

Detect gas through which jets travel **while decelerating** (also enhanced X-rays on jet path):

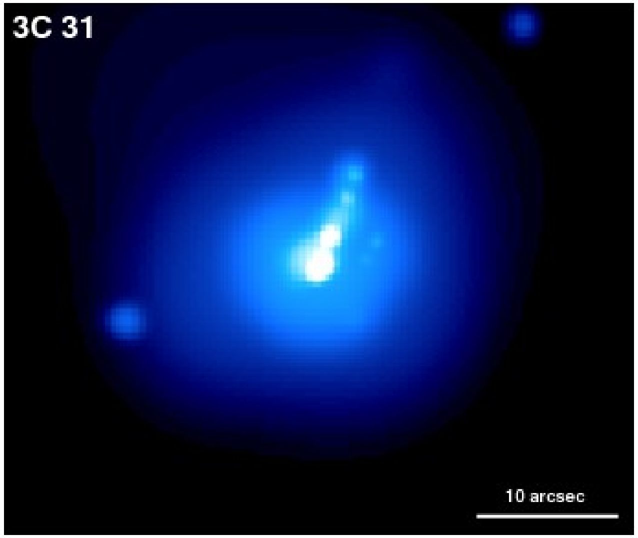

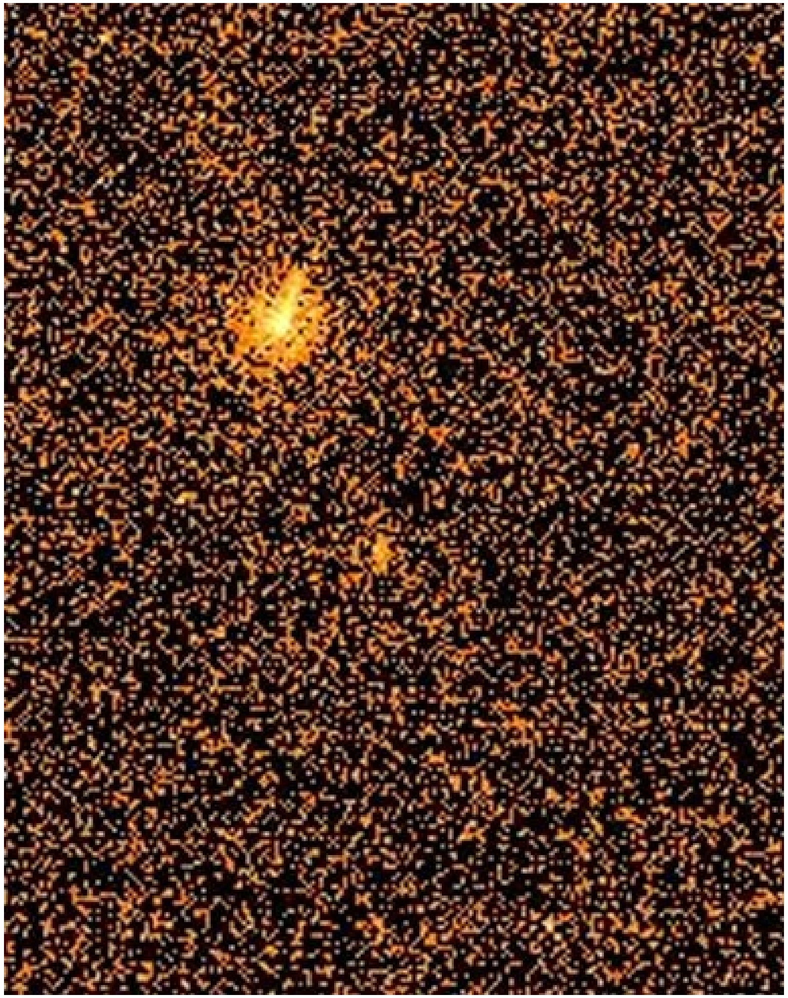

0.5 to 7 keV Chandra image
Hardcastle et al. MNRAS 334, 182 (2002)

Conservation Law Analysis

- Energy Flux conserved

$$\Phi = [(\Gamma^2 - \Gamma)\rho c^2 + 4\Gamma^2 p]\beta c A$$

- Momentum Flux conserved (buoyancy effect included)

$$\Pi = [\Gamma^2\beta^2(\rho c^2 + 4p) + p - p_{\mathrm{ext}}]A + \int_{r_1}^{r} A\frac{\mathrm{d}p_{\mathrm{ext}}}{\mathrm{d}r}\left[1 - \frac{\Gamma^2(\rho c^2 + 4p)}{c^2(1+\beta^2)\rho_{\mathrm{ext}}}\right]\mathrm{d}r.$$

- Find solutions for jet pressure, density variation with given energy, momentum fluxes constrained by known external pressure and density from X-ray data. Assume $p \rightarrow p_{ext}$ in outer jet and Energy Flux = (Momentum Flux x c) on small scales
  [Laing and Bridle MNRAS, 336, 1161 (2002)]

Mass Loading (1)

Injection by stellar winds within volume swept by jet flow

Komissarov (1994) MNRAS 269, 394

Bowman, Leahy & Komissarov (1996) MNRAS 279, 899

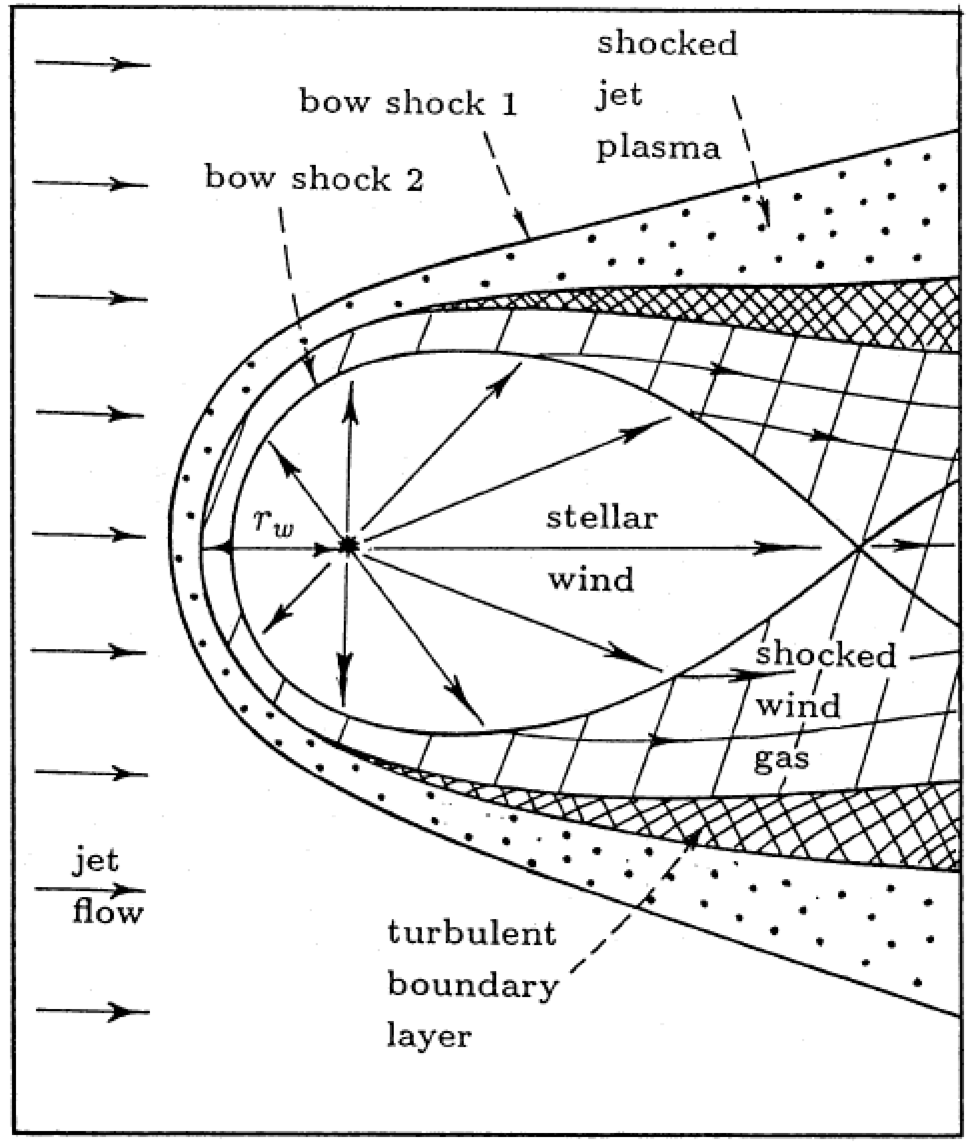

Figure 1. The interaction between the jet and the stellar wind. Because both the flows are supersonic, a double-bow-shock configuration is formed.

Mass Loading (2)

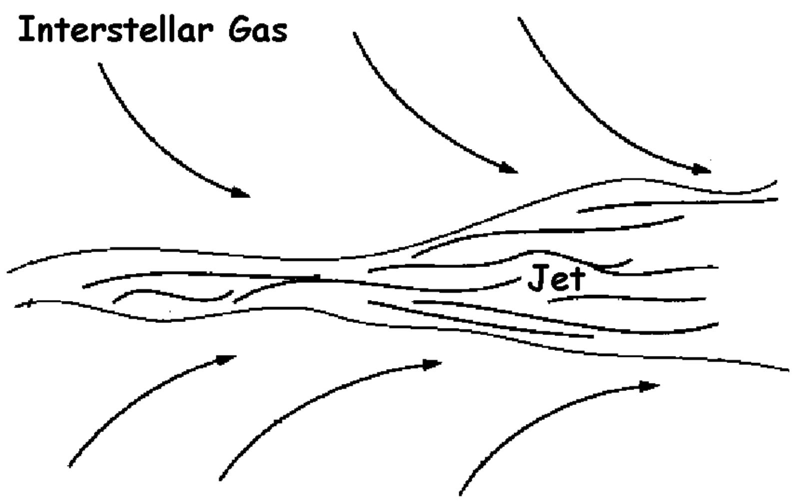

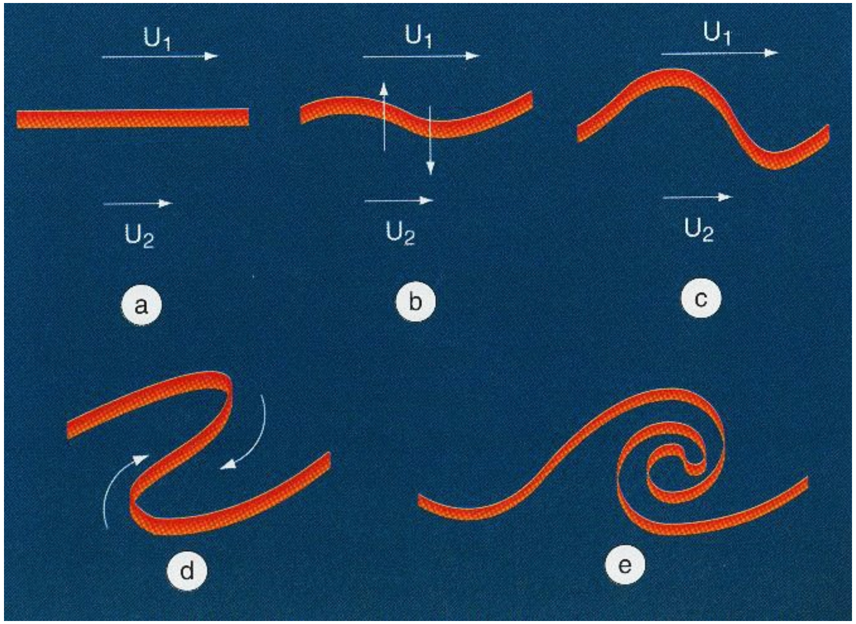

Ingestion of ambient galactic ISM by eddies in the turbulent boundary layer of jet (K-H instability) (De Young 1996)

Mixing Layers in Lab Jets

(N.B. non-relativistic, non-magnetic!)

- Thickness grows with distance/time

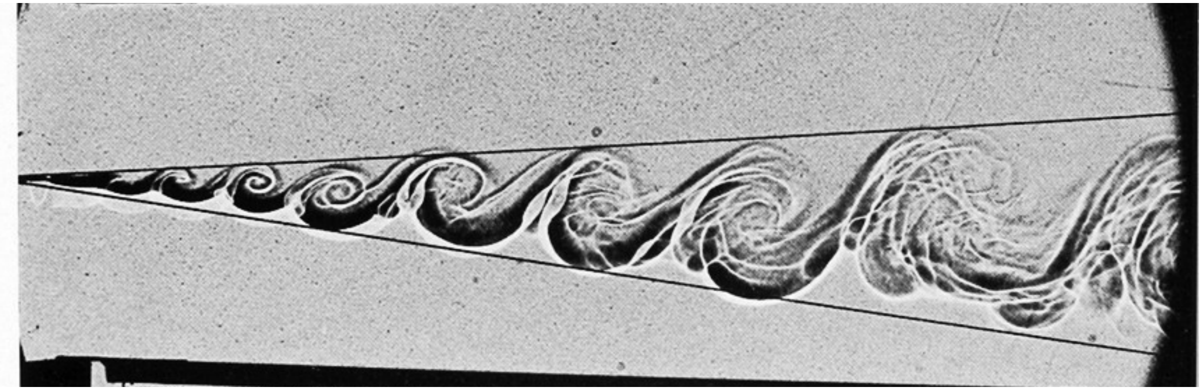

$$\mathrm{Tan}\,\phi = C\,(\rho_L/\rho_H)^{\alpha}\,(v_{REL})^{-\beta}$$

- Layer can grow to fill jet

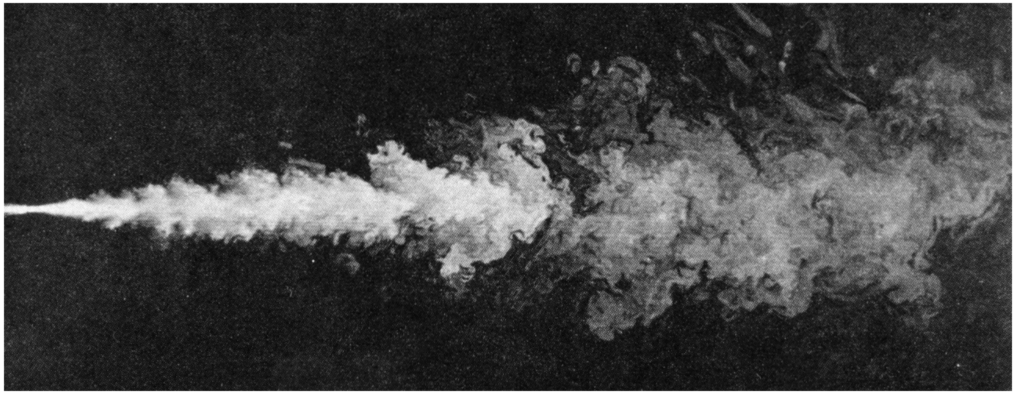

Relativistic Jet Boundary Layers

3-D RHD: Aloy et al. ApJ, 523, L125 (1999)
- note RMHD effects depend on toroidal/poloidal field configs

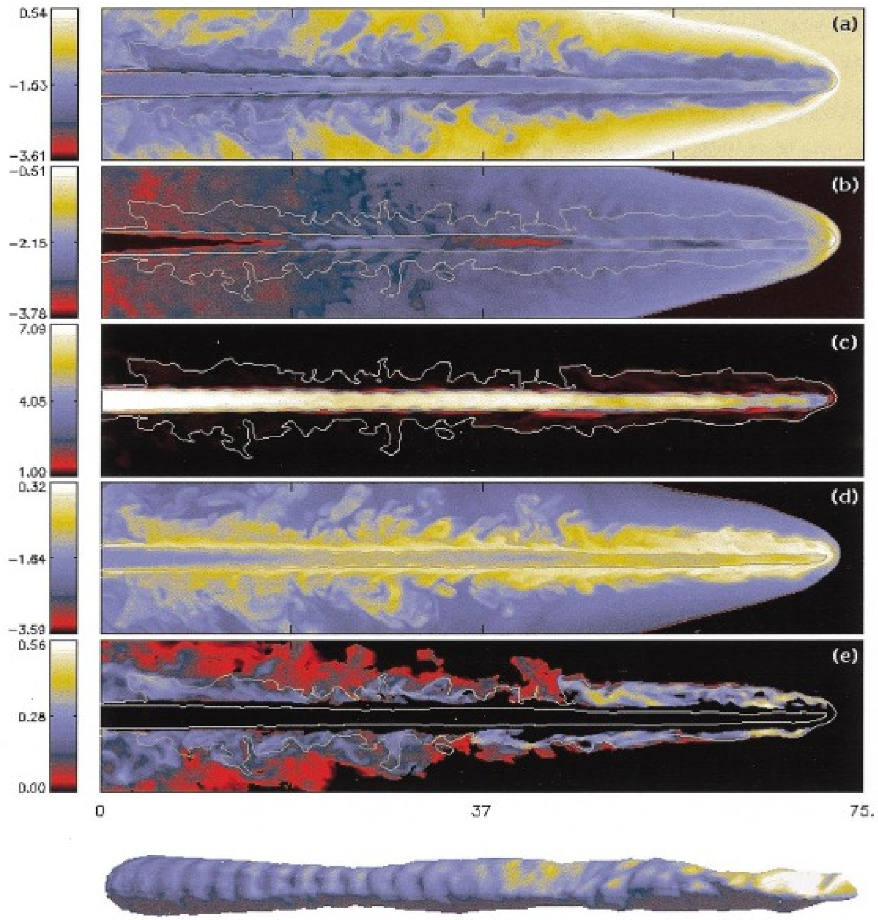

FIG. 1.—(*a*) The rest-mass density, (*b*) pressure, (*c*) flow Lorentz factor, (*d*) specific internal energy, and (*e*) backflow velocity distributions of the model discussed in the text in the plane $y = 0$ at the end of the simulation. The white contour levels appearing in each frame correspond to values of $f = 0.95$ (*inner contour*; representative of the beam) and 0.05 (representative of the cocoon/shocked external medium interface). The bottom panel displays the isosurface of $f = 0.95$.

Entrainment Rate into 3C31 Jet

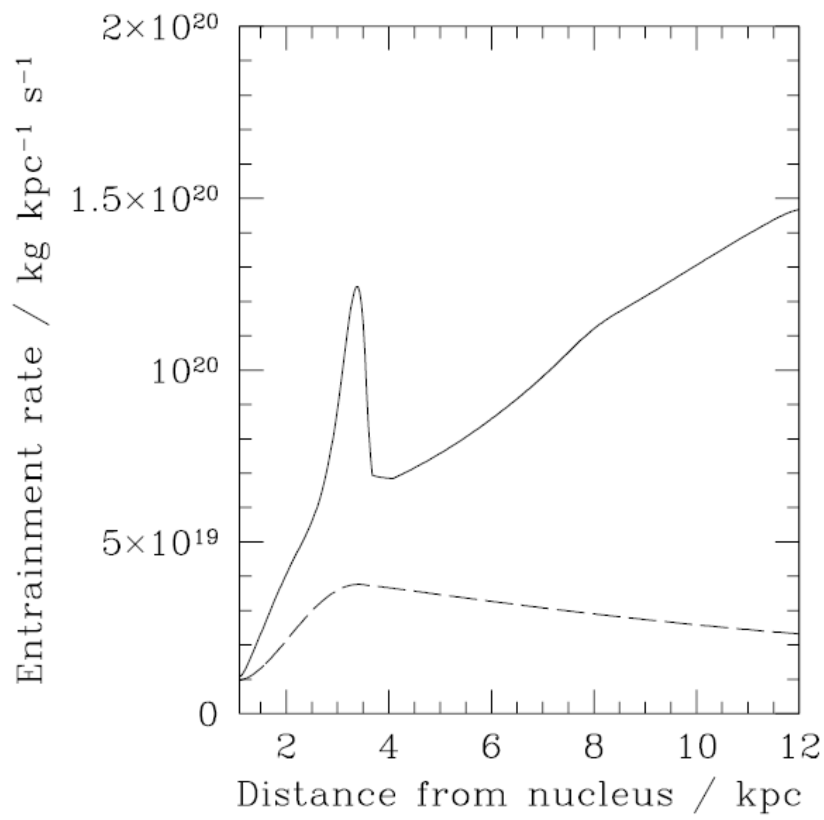

Figure 11. The estimated internal mass input rate from stars (long dashes) superimposed on the entrainment rate required by the reference model (full line).

consistent with light (e.g. electron-positron) jet that is mass-loaded by stellar injection in first kpc, then decelerates rapidly by ingestion of ISM across jet boundary

Laing and Bridle MNRAS 336, 1161 (2002)

Entrainment Rate into NGC315 Jet

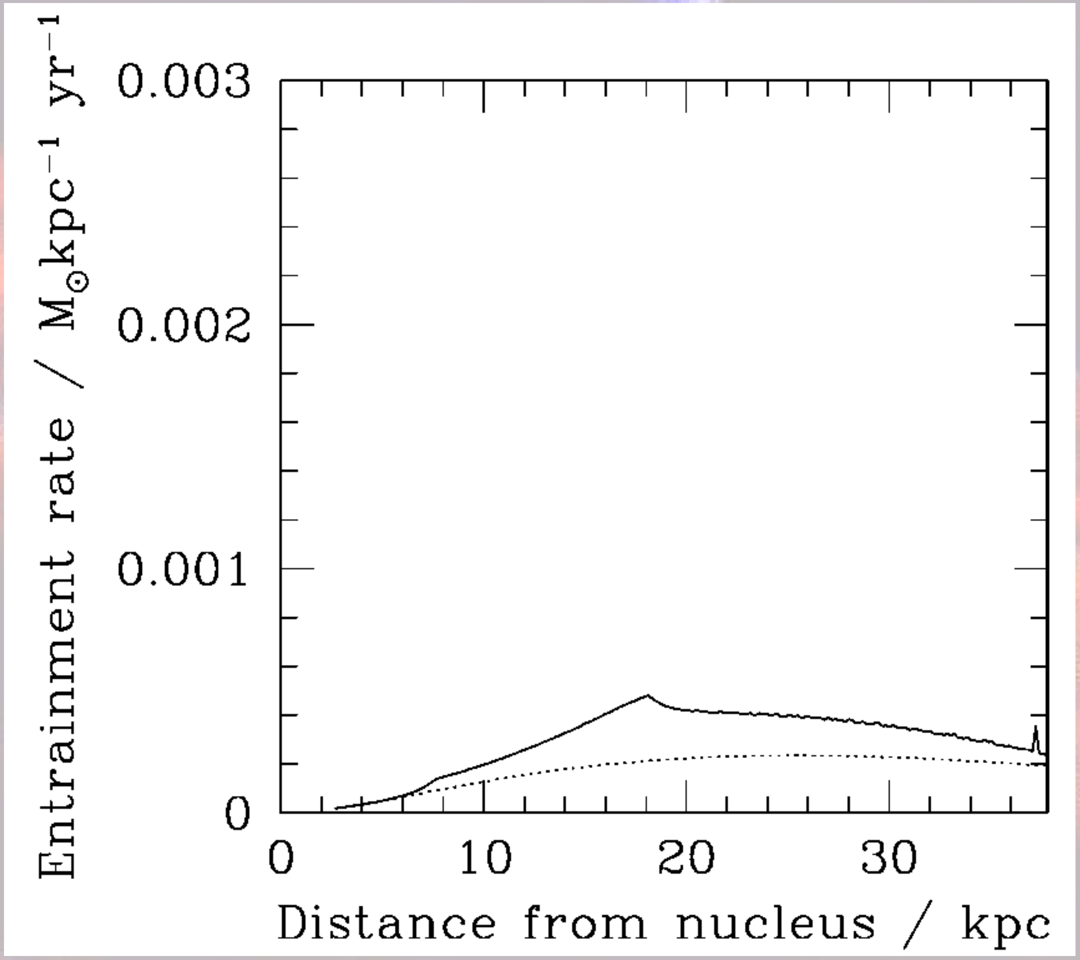

consistent with light jet that is mass-loaded by stellar injection

Laing, Canvin and Bridle in preparation (2006)

Adiabatic Jet Assumptions

- Energies of particles scale as $V^{-1/3}$
- No diffusion
- Particle momentum distribution remains isotropic
- B-field behaves as if passively convected with flow
- Synchrotron and inverse Compton losses negligible

With these assumptions, parameters at any jet cross-section given a model velocity field, determine those everywhere

Adiabatic deceleration?

Laing and Bridle MNRAS 348, 1459 (2004)

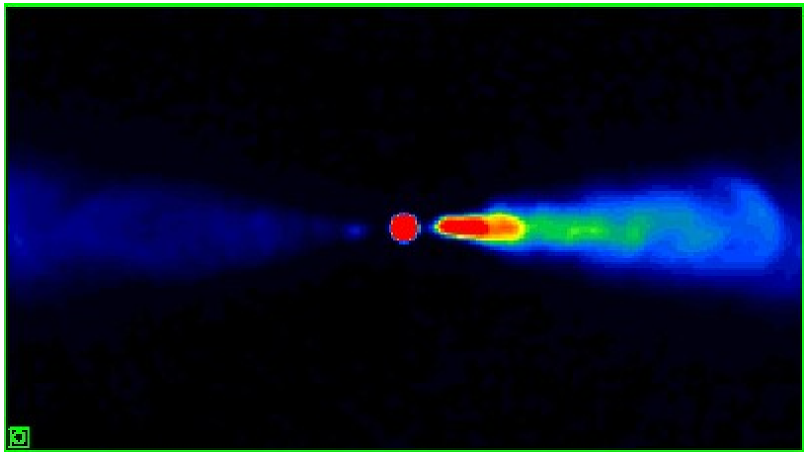

3C 31 observed

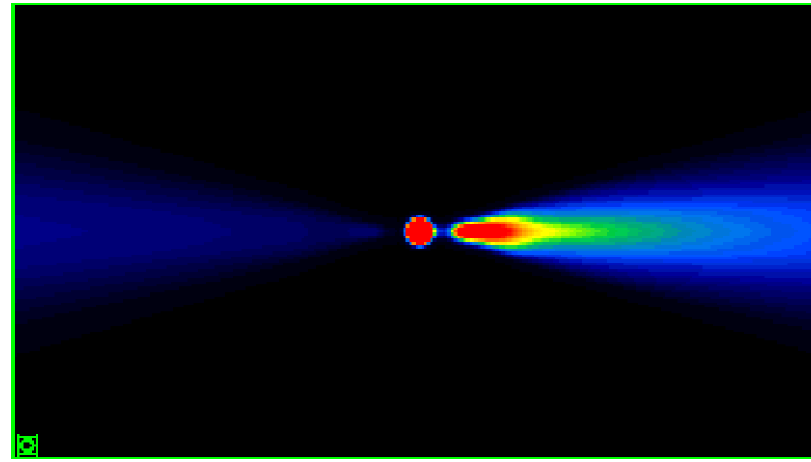

“Free” model fit

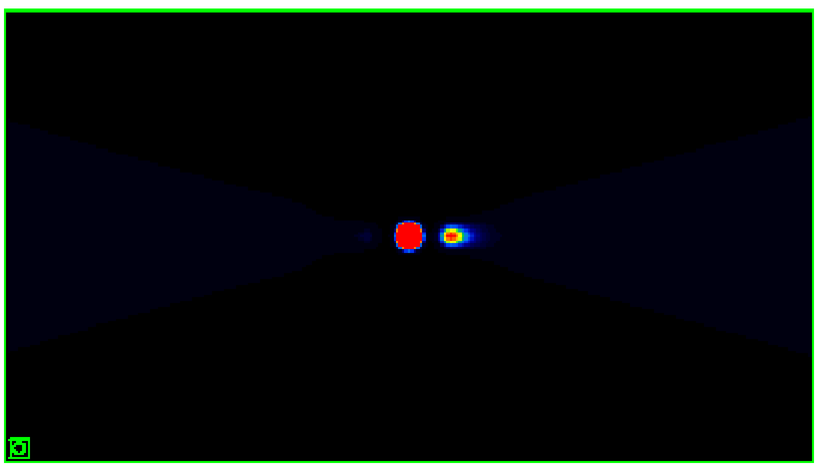

Adiabatic jet with velocity and initial conditions in free model

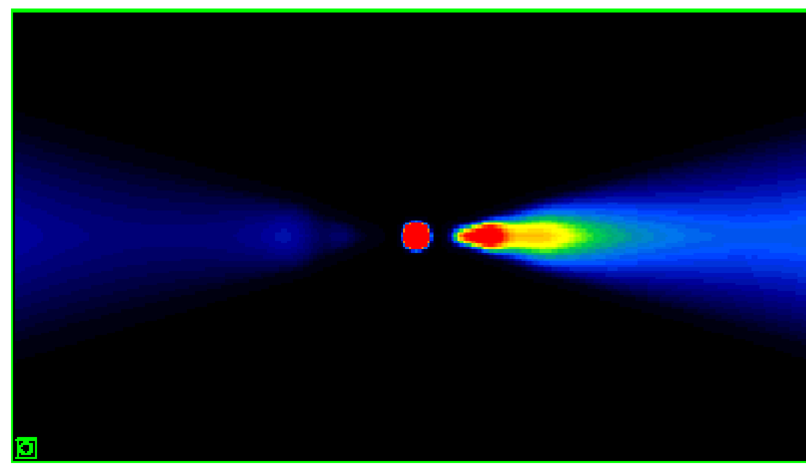

Adiabatic + distributed rel. particle injection

3C31 radio and X-ray superposed

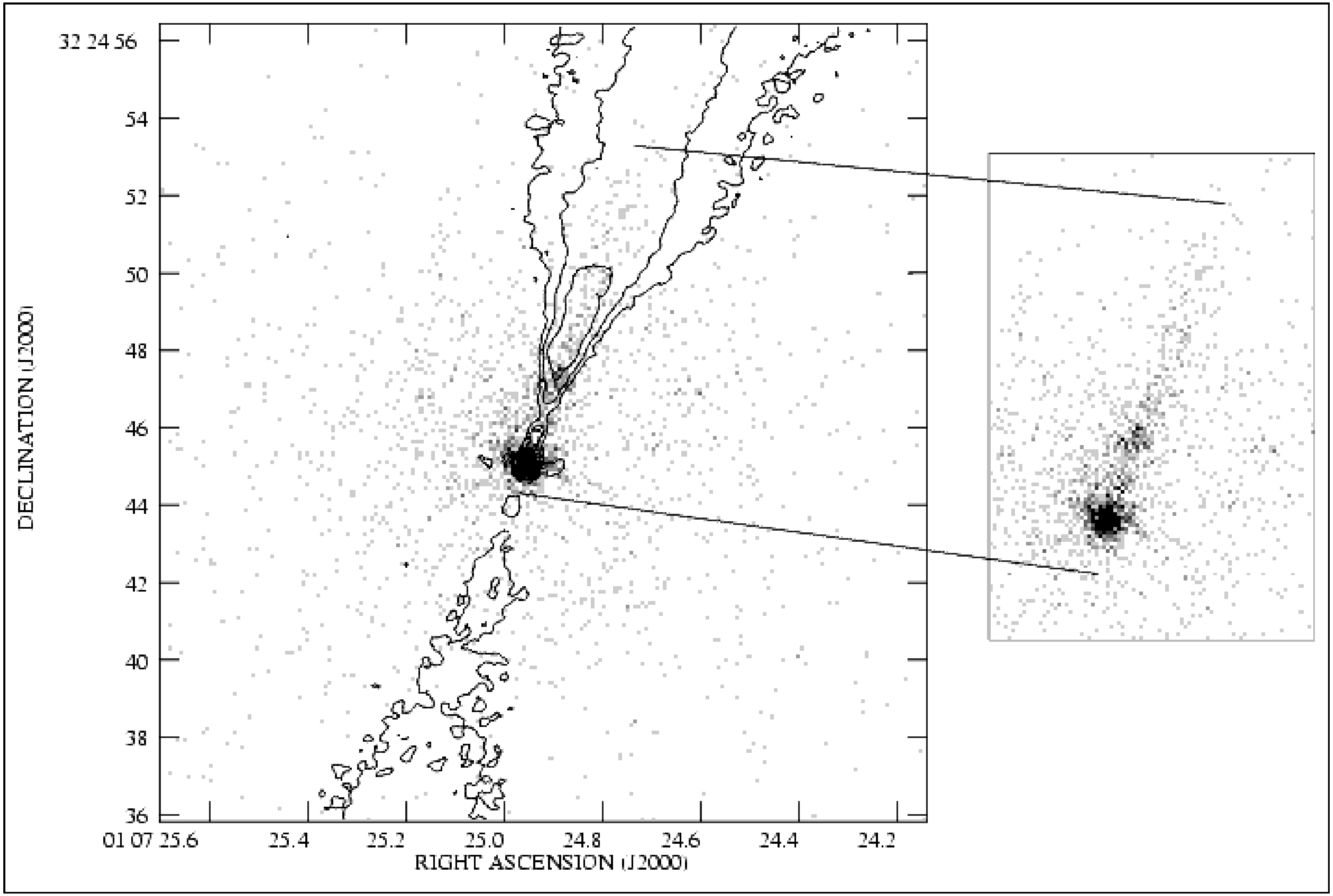

8.4 GHz VLA

0.5 to 7 keV Chandra

Where are particles injected?

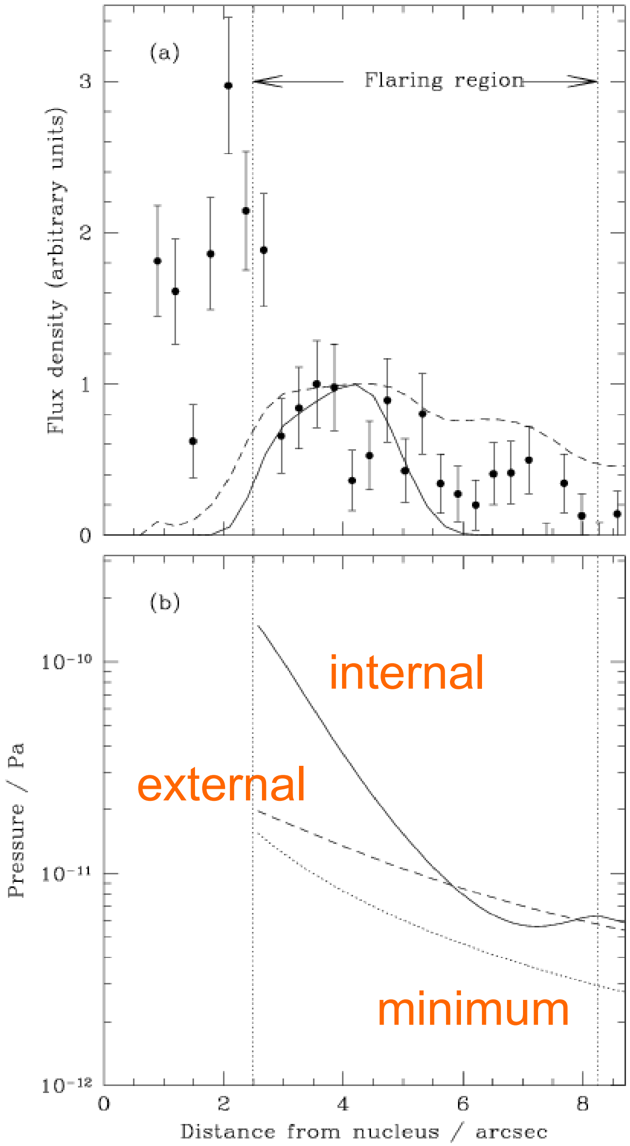

Points – X-ray

Full line – particle injection function required by fit

Dashed - radio

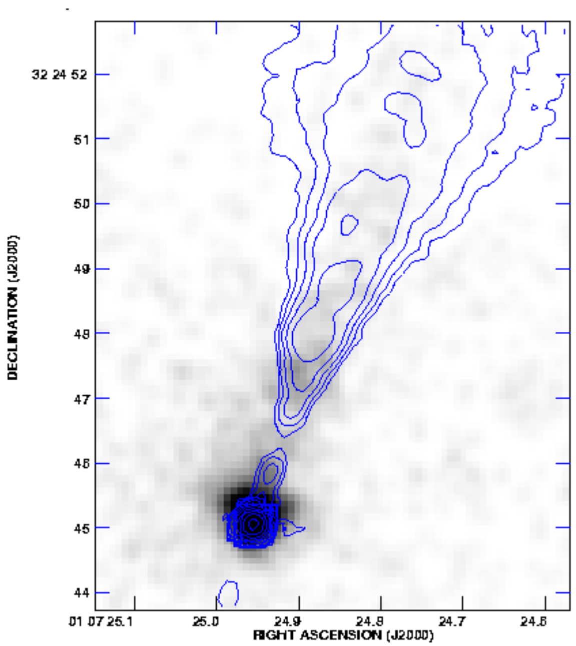

Pressures from conservation-law analysis

Laing and Bridle MNRAS 336, 1161 (2002)

Family resemblances in FR1 jets

- Jets at <1 kpc have v>0.8c, slow expansion rate
- Jets decelerate rapidly to 0.1 to 0.4c in region of fast lateral expansion (flaring)
- Slower velocities on jet boundaries than on jet axis (transverse velocity shear)
- Jet B-field evolves from predominantly longitudinal close to nucleus to predominatly toroidal further out; radial component generally small (suppressed by velocity shear?)
- Jets intrinsically center-brightened
- Particle injection in flaring region, quasi-adiabatic evolution further out

Input to guide R(M)HD Jet Simulations

e.g. Perucho (Michigan Relativistic Jets Conference Dec 2005)

2D attempt to reproduce 3C31 dynamics deduced from VLA/Chandra data

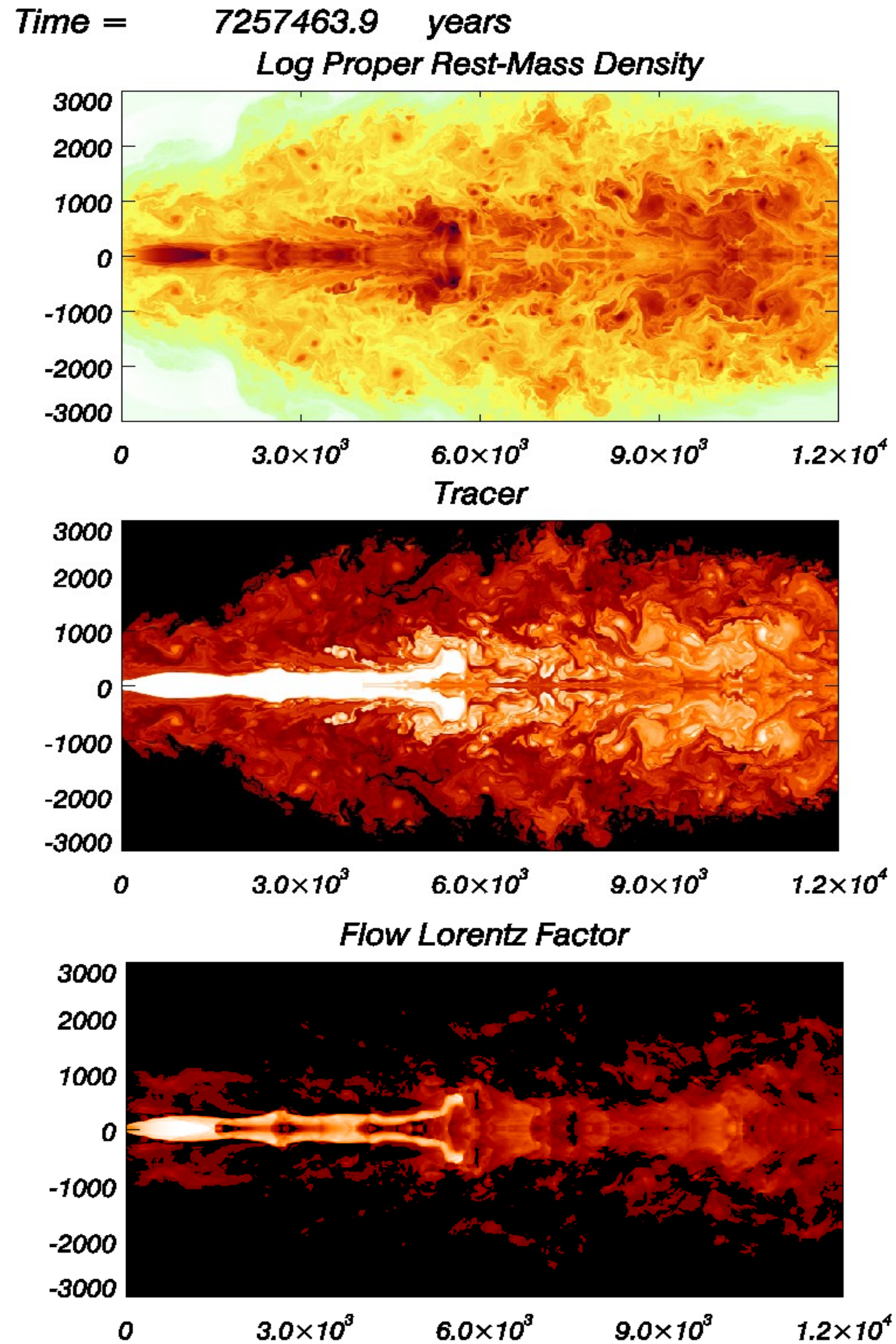

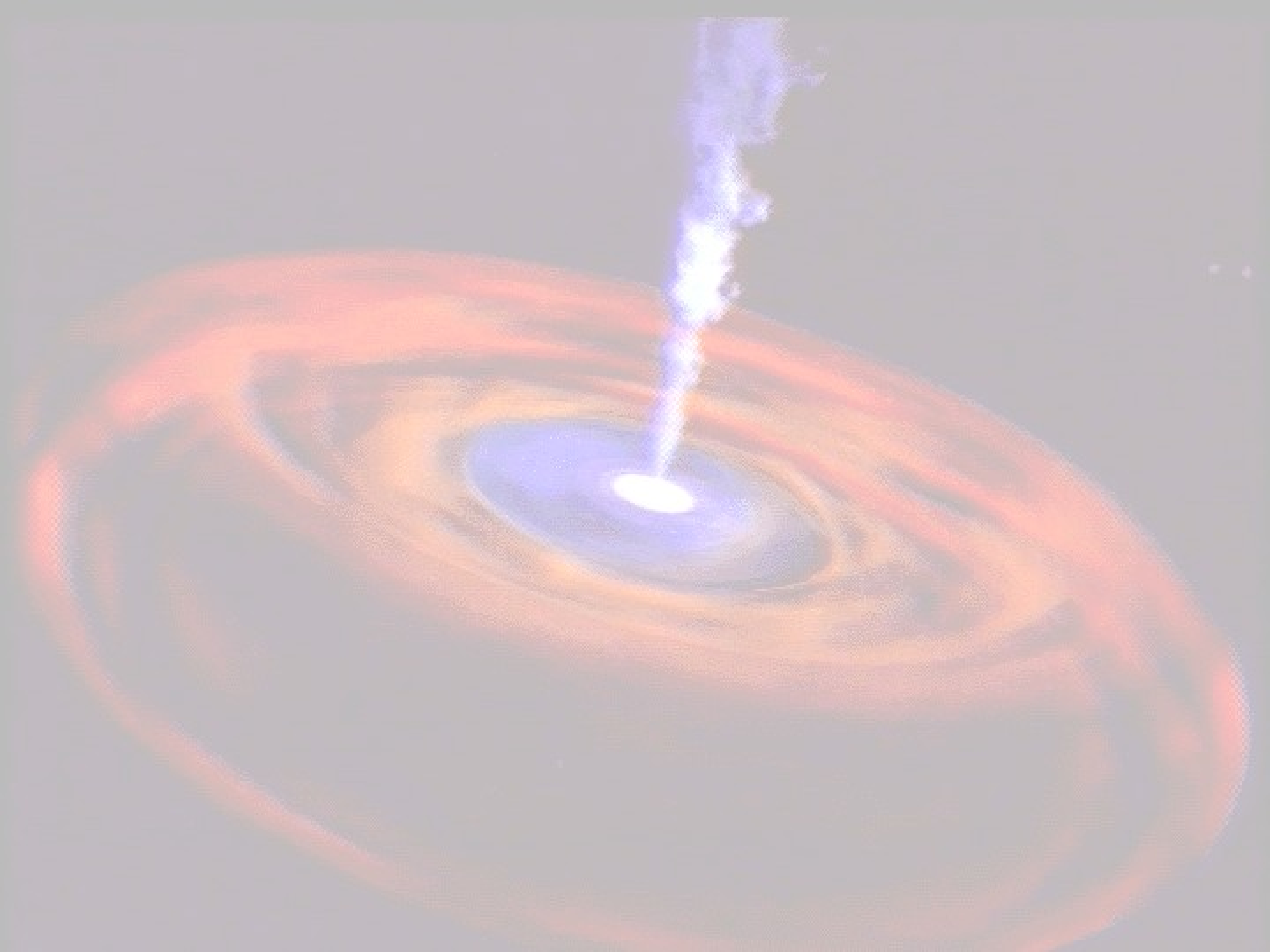

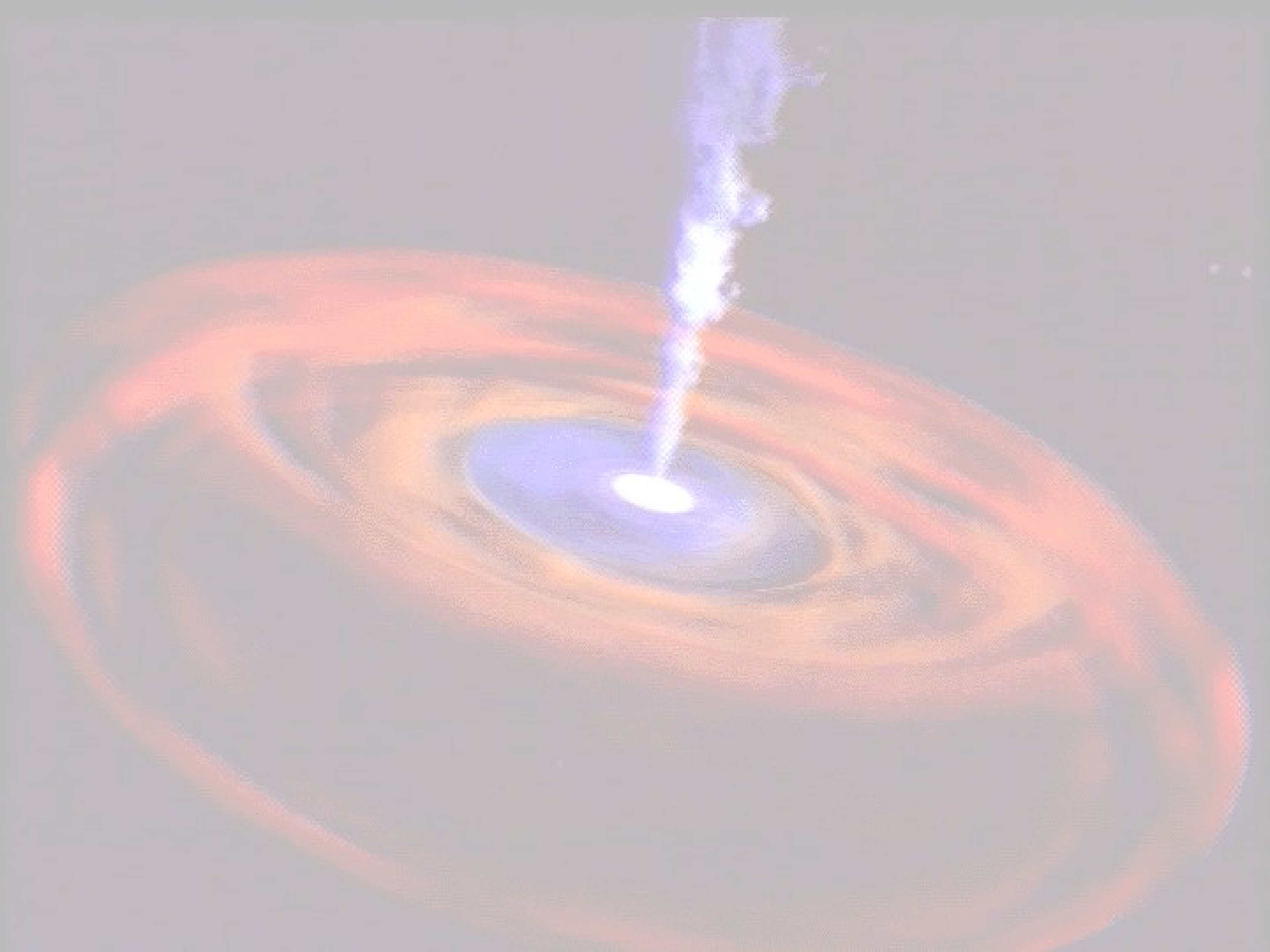

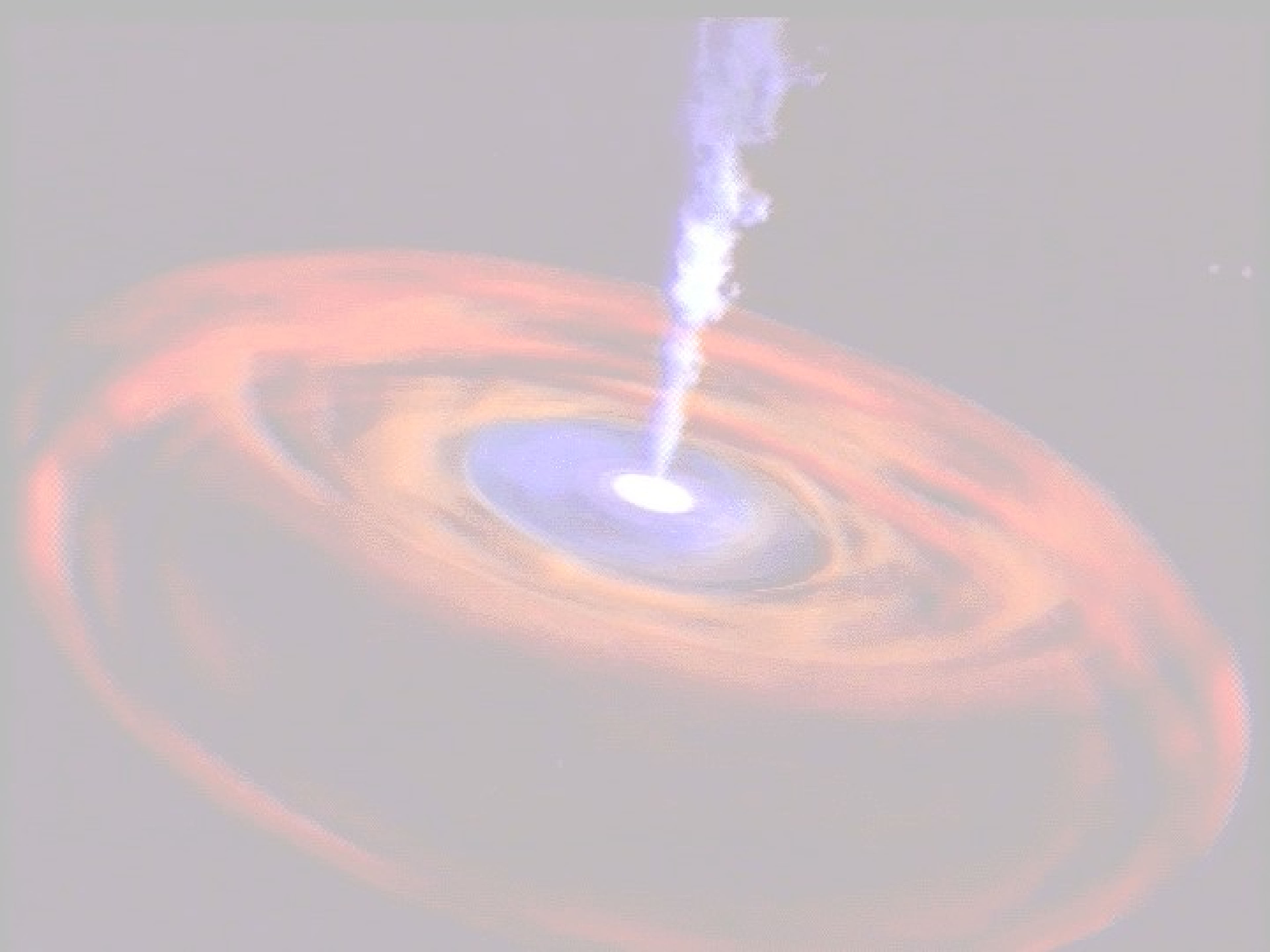

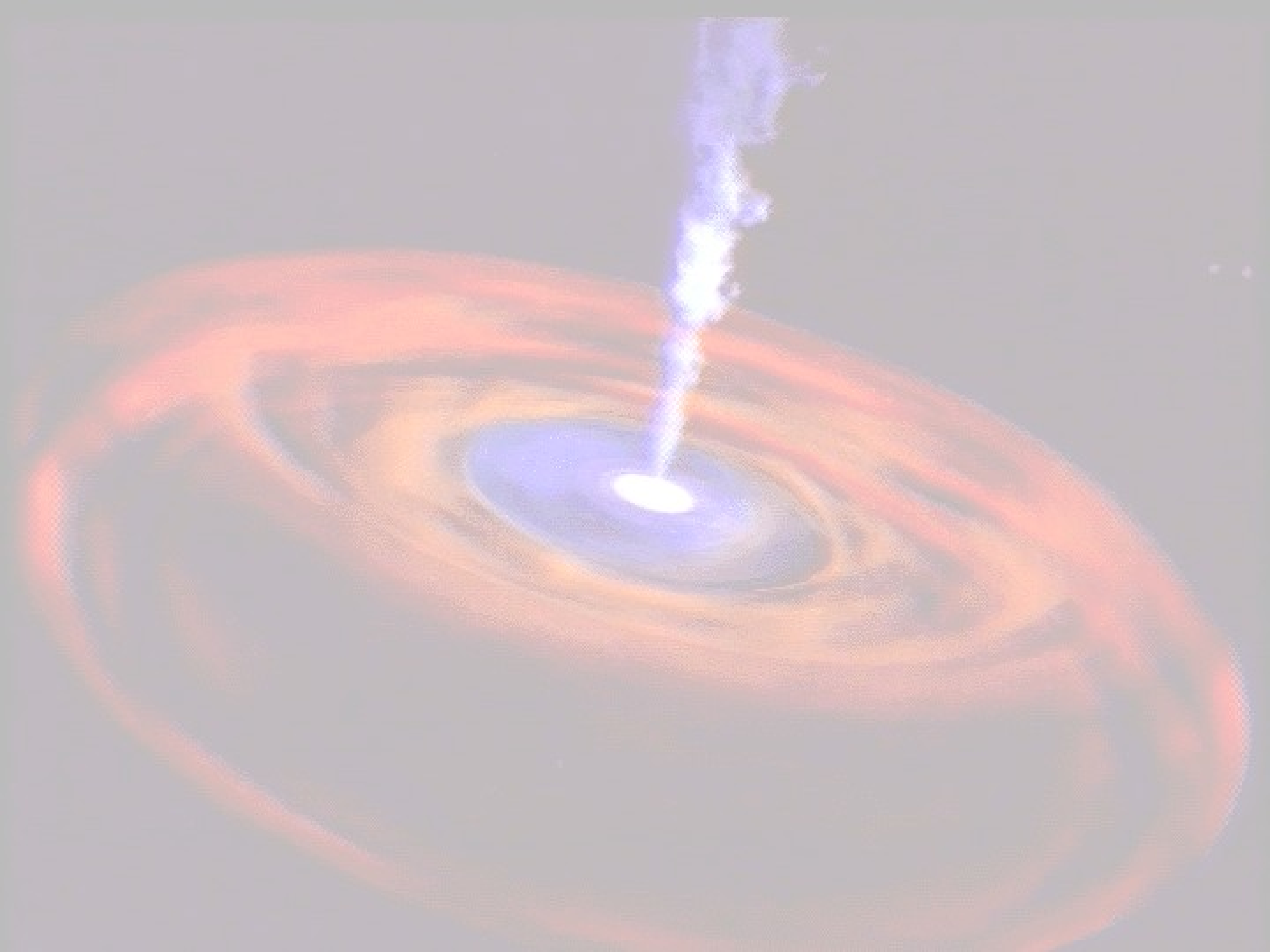

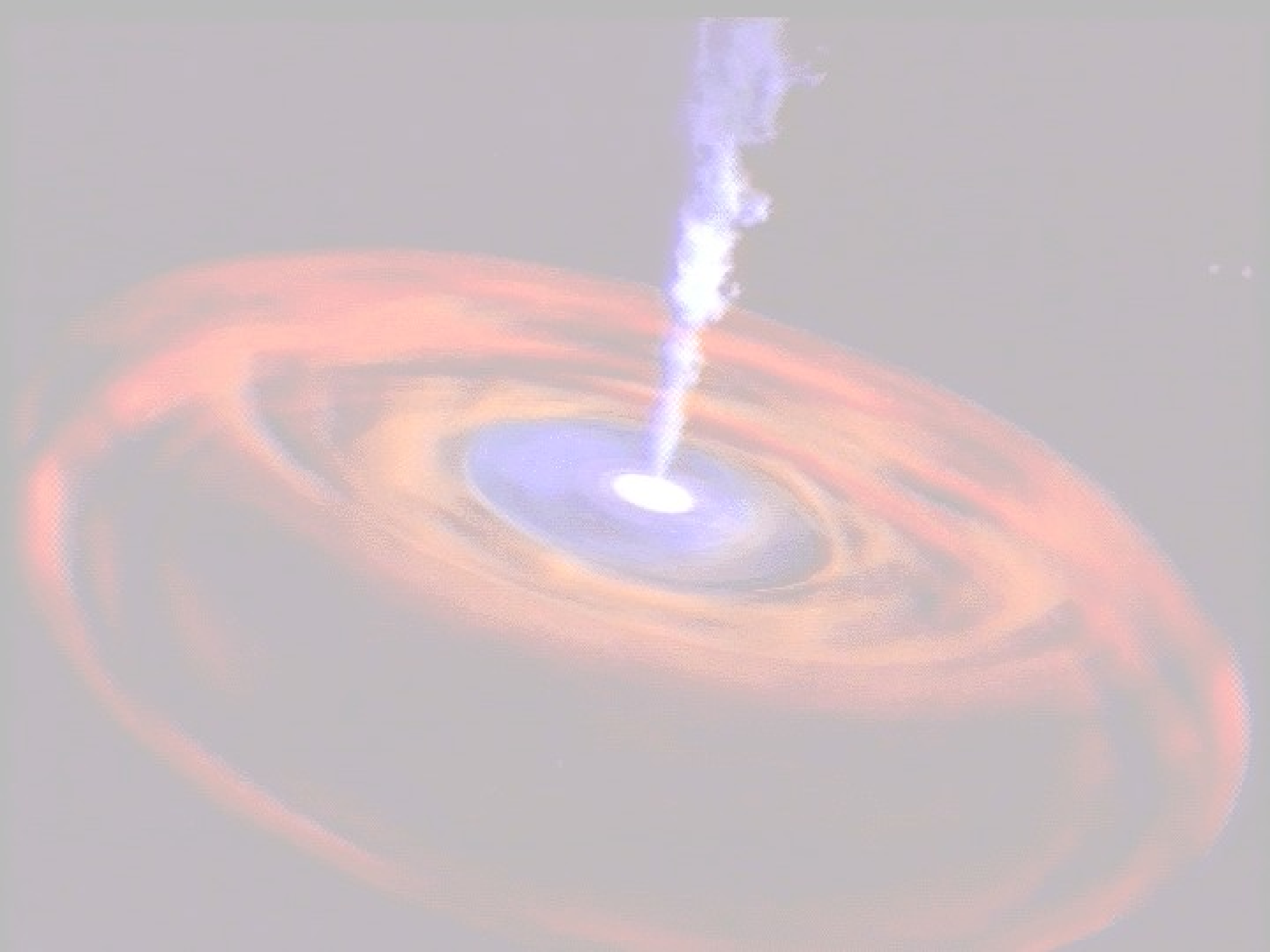

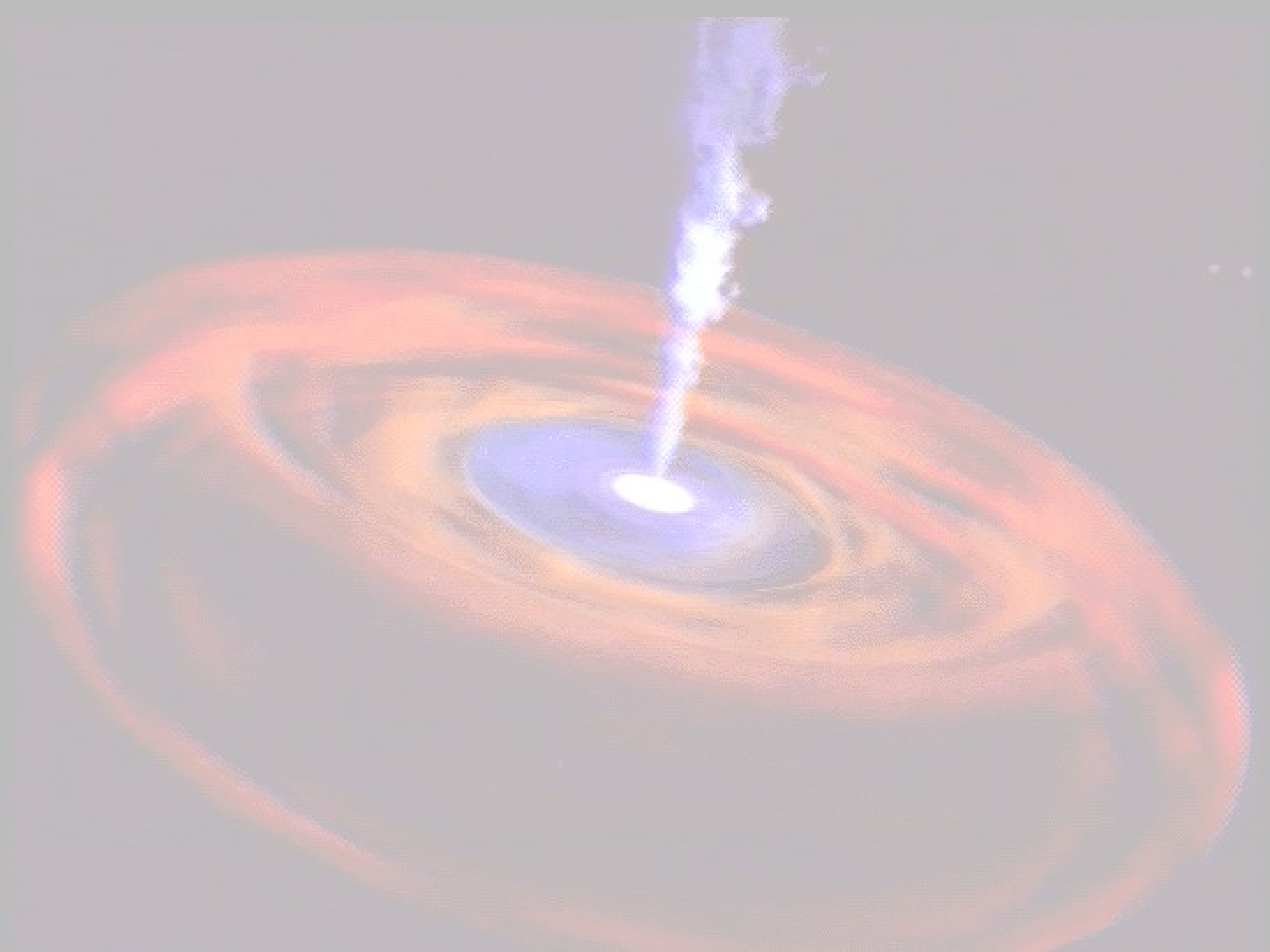

M87